

Historical perspective

Variations in foam collapse and thin film stability with constant interfacial and bulk properties

Peter Alexander Wierenga ^{a,*}, Elke Simeonova Basheva ^b, Roy Jozef Bernard Marie Delahaije ^a^a Laboratory of Food Chemistry, Wageningen UR, Bornse Weilanden 9, Wageningen 6708, WG, the Netherlands^b Department of Chemical and Pharmaceutical Engineering, Sofia University, Bulgaria

ARTICLE INFO

Keywords:

Thin film balance
Dilatational surface viscoelasticity
Dynamic surface tension
Protein
Beer
Capillary cell

ABSTRACT

The stability of foams is commonly linked to the interfacial properties of the proteins and other surfactants used. This study aimed to use these relationships to explain differences in foam stability observed among similar beer samples from different breweries. The foam stability was different for each sample (Nibem foam stability ranged from 206 to 300 s), but ranking was similar for all three foaming methods used, thus independent of the method, gas, etc. Differences in foam stability were dominated by differences in coalescence, as illustrated by the correlation with the stability of single bubbles and thin liquid films. The differences in coalescence stability could not be explained by the measured interfacial properties (e.g. surface pressure, adsorption rate, dilatational modulus and surface shear viscosity), or the bulk properties (concentration, pH, ionic strength, viscosity), since they were similar for all samples. The drainage rates and disjoining pressure isotherms measured in thin liquid films were also similar for all samples, further limiting the options to explain the differences in foam stability using known arguments. The differences in coalescence stability of the thin films was shown to depend on the liquid in between the adsorbed layers of the thin film, using a modified capillary cell to exchange this liquid (to a buffer, or one of the other samples). This illustrates the need to review our current understanding and to develop new methods both for experimental study and theoretical description, to better understand foam stability in the future.

1. Current view on foam stability

It is sometimes important to reflect on the concepts and theories used in a certain scientific field, and on the available experimental evidence to support them. This is for example relevant when considering foams stabilised by proteins or low-molecular weight surfactants. There is a large body of literature on the relation between foam properties and interfacial properties of proteins and other surfactants, e.g. [1–9]. When reading this literature, it becomes clear that there is an established consensus on the mechanisms that are important in foam stability. In short, proteins need to adsorb to the interface, leading to a decrease in interfacial tension and increase of interfacial elasticity. After the foam is formed, it destabilises through disproportionation and/or coalescence of bubbles. Both processes are influenced by the thickness of the thin films separating the bubbles, and thereby they depend on the drainage of liquid. The drainage is influenced by bulk viscosity, disjoining pressure and interfacial rheology.

For some proteins (and protein hydrolysates), a correlation between

certain interfacial properties and foam stability (collapse) was reported [10–12]. A closer inspection of literature, however, easily shows the lack of proof for a (consistent) quantitative relationship between the absolute values of properties of the adsorbed layers, or thin films and the foam stability. This lack has also been mentioned in some review articles [8,13]. For β -lactoglobulin, Gochev et al. concluded that the increasing (foam) film stability with increasing pH could not be explained by the adsorption and surface viscoelastic properties of the adsorbed layers [14]. The lack of proof is in part due to the fact that only few studies have covered experiments at the different length scales, i.e. single interfaces, thin films, and foam. Therefore, this study aims to include experiments on all relevant length scales to evaluate if the presumed relationship between interfacial and foam properties can be used to explain differences in foam stability observed among batches of similar beer samples from different breweries.

* Corresponding author.

E-mail address: peter.wierenga@wur.nl (P.A. Wierenga).

1.1. Different length scales in foam formation and stability

The understanding and description of foam requires a description of the system on different length scales (Fig. 1). A macroscopic foam contains a large number of bubbles, separated by thin liquid films. The liquid in the thin films will drain to the Plateau borders until it reaches the bulk liquid below the foam. The drainage has been studied in thin liquid films formed in a capillary or Mysels (porous) cell (also sometimes called the thin film balance and thin film pressure balance), and by a single bubble captured under an interface [15]. The interface of each bubble is covered by adsorbed proteins or other surfactants. To study the properties of these adsorbed layers, measurements can be done on single interfaces, for instance using a drop tensiometer [11]. These techniques have largely increased our knowledge and understanding of the phenomena on the various length scales. There is however still a large step in complexity when going from adsorption at air-water interfaces (e.g. as measured by drop shape analysis) to foam stability (e.g. decrease of foam height versus time). This large step in complexity may have contributed to the difficulties in making the relation between the experiments on smaller length scale and final foam stability.

Another challenge in this field, especially protein stabilised foams, may have been that the actual amount of published experimental data on foam *stability* is relatively limited, more papers focus on foam *ability* (formation). In addition, for some articles in which foam stability data was provided the stability of the foam against *drainage* was measured [11,16,17]. There are only few articles reporting on the change of foam height versus time (foam collapse), which also hindered identification of quantitative description of foam stability linked to the relevant processes and parameters, as discussed further below.

1.2. Foam formation and adsorption kinetics

The foam ability describes how much foam is formed from a protein solution under given condition and after a certain time of foaming (e.g. sparging). The foam ability of a solution has been linked to the initial rate of surface pressure increase, $d\Pi/dt$ [2,13,18–20]. This parameter can be seen as an apparent adsorption rate, but it is of course only an indirect indication of the real (initial) adsorption rate measured as the increase in adsorbed amount in time, $d\Gamma/dt$. Experimentally, the link

between (apparent) adsorption kinetics and foam ability was shown by increasing the protein concentration [21–26], changing the type of protein [10,24,25], or the system conditions (pH, ionic strength) [23–25,27]. In each of these cases, the increased adsorption kinetics resulted in an increased foam ability, and a decrease in average bubble size ($d_{3,2}$), until at some point the maximum foam ability and minimal bubble size were obtained, shown in detail in [22,23]. All these data have clearly shown the qualitative link between adsorption kinetics and foam formation. There is at this moment, however, no quantitative relation to link adsorption kinetics to foam volume, or bubble size as has been proposed for emulsions [28].

1.3. Foam stability and interfacial properties: theoretical description

Depending on the study, foam stability is either referred to as stability against drainage or stability against collapse. Stability against drainage is measured by the loss of liquid from the foam. Stability against collapse is typically measured by the decrease in foam height due to coalescence and/or Ostwald ripening. Drainage will occur from the moment the foam is formed, resulting in thinning of the liquid films separating the bubbles. Coalescence and Ostwald ripening are accelerated by the decreasing film thickness, and result in collapse and coarsening of the foam. All these processes have been mentioned in numerous reviews to depend on the interfacial rheological properties, i.e. surface viscosity or elasticity [3,5,6,9,13,29–31]. Noskov et al. showed that the surface elasticity for pure proteins was affected by denaturation [32–34]. In other studies, they describe the decrease of surface elasticity in mixed protein-surfactant systems [35,36]. For pure protein systems typically a high dilatational elastic modulus is considered essential to obtain a (very) stable foam [37]. However, upon closer inspection, it became clear that it was not always made explicit by which mechanisms or to which extent exactly the interfacial rheology was considered to influence the foam stability. In the sections below the main arguments provided in literature are given.

1.3.1. Drainage

The drainage in thin films is driven by the difference between the pressure in the Plateau borders and the forces separating the two air-water interfaces in the thin films; the disjoining pressure (Π). The

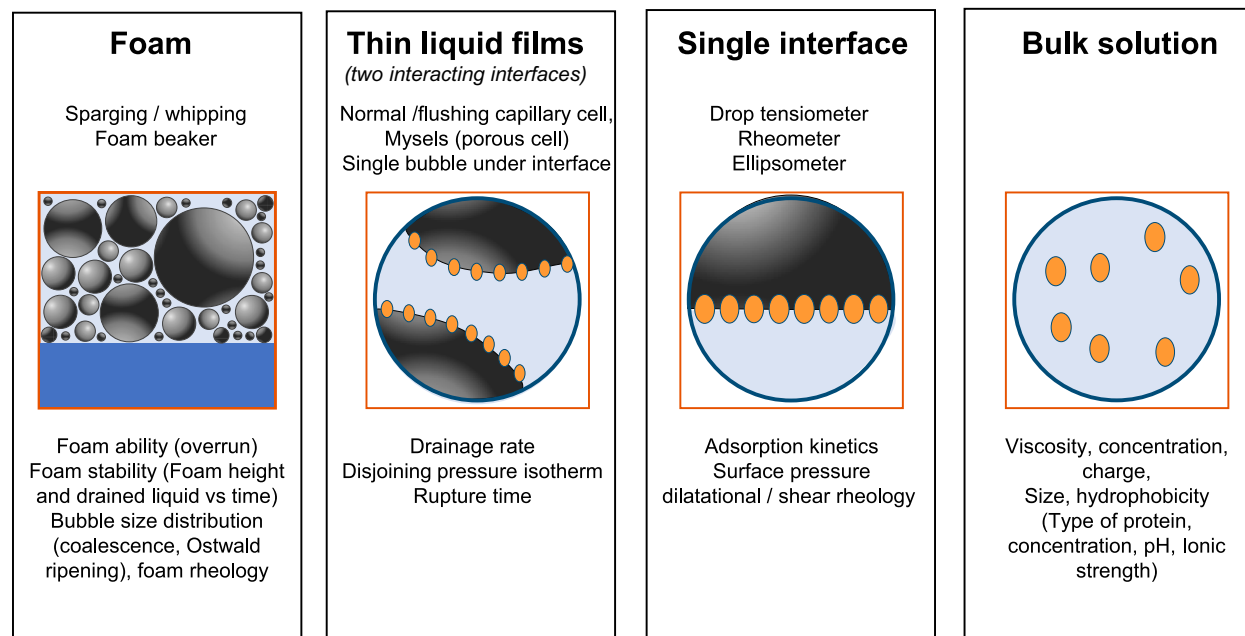


Fig. 1. Overview of the different length-scales relevant in foam studies, with a description of methods applied to study the system at the different scales and the relevant parameters that can be derived from such analyses.

drainage rate, as given in Eq. (1), depends on the thickness and radius of the film, viscosity of the liquid, the surface mobility and the disjoining pressure [5,38–40].

$$\delta h / \delta t = -2c_f h^3 / 3\mu R_f^2 (\gamma / R_p - \Pi) \quad (1)$$

Where h is the film thickness, R_f the film radius, μ the liquid viscosity and the constant c_f accounts for the mobility of the interfaces. For immobile surfaces, such as protein stabilised surfaces $c_f = 1$ [5]. Film thinning is driven by the difference in Laplace pressure of the adjacent Plateau borders γ / R_p and the film disjoining pressure Π , where γ is the surface tension and R_p the radius of the plateau border. For low-molecular weight surfactants, there is typically a very low surface elasticity, and high surface viscosity. This results in Marangoni flow when there are surface tension gradients at the interface. Such gradients can be induced by liquid drainage in the thin films. For adsorbed protein layers, the interfacial mobility is typical zero [41], so in protein stabilised surfaces the Marangoni flow is considered to be absent/negligible. As a consequence, no significant contribution of surface rheological properties on the drainage rate is expected. As a result, for such systems, the drainage rate in different foams will be determined by differences in bubble size, bulk viscosity, surface tension and disjoining pressure.

1.3.2. Ostwald ripening

Ostwald ripening is driven by a reduction of the total surface area and thereby the interfacial energy [42]. Since Ostwald ripening involves diffusion of gas through a liquid, an important factor influencing the rate of Ostwald ripening is the gas solubility. As a consequence, Ostwald ripening can be retarded by using a gas with a lower solubility such as nitrogen instead of carbon dioxide [43]. Moreover, it has been suggested that Ostwald ripening could be prevented through the elastic properties of the interface. It has, however, been shown that for adsorbed protein layers with a viscous behaviour Ostwald ripening is only retarded, and not stopped [44].

1.3.3. Coalescence

The last point where interfacial rheology could be important for foam stability is coalescence, which is the rupture of the thin liquid films separating the bubbles. The rupture of thin liquid films is typically considered to occur once a critical thickness is reached, the argument is also referred to as the Vrij criterion [5,45]. There is a very large body of literature on the stability of thin liquid films, see for example [5,9,13,31,39,45–56]. The *possible mechanism* (sic.) proposed by Vrij assumes that certain perturbations in film thickness will occur due to for example thermal fluctuations. The growth of these thickness fluctuations will depend on the same properties that also determine the drainage rate (i.e. viscosity, disjoining pressure, surface tension) [45]. There are also arguments that the surface rheological properties should be included in this analysis [5,57]. To include the surface elastic modulus, Meinders et al. [5] suggested the following expression for the Vrij criterion (Eq. (2)):

$$\delta \Pi / \delta h < -\pi(\gamma + E_d) / R_f^2 \quad (2)$$

Where γ is the surface tension and E_d the surface dilatational elastic modulus. The disjoining pressure is the result of van der Waals, electrostatic and oscillatory forces between the two interfaces of the thin film [5,55,56,58]. However, Sheludko already remarked that “*Rupture is not observed when a stable structure is formed at thickness below the critical thickness*”, and “*There is also the fact that films which do rupture nevertheless exist for a certain time before rupture occurs*” (sic.) [55]. Previously, Charles also observed that “*films may rupture at different thicknesses*” (sic.) [59]. Both comments indicate that perhaps the concept of critical thickness is too absolute, and that in reality sometimes films may drain until a thickness where the films rupture after a certain time, i.e. stochastically. This concept was elaborated by Chatzigiannakis who

proposed that the thin films may rupture either according to the deterministic or stochastic theory, depending on the exact conditions in the film [60].

1.4. Foam stability and interfacial properties: experimental evidence

A link between surface rheology and foam stability against collapse was shown experimentally for low molecular weight surfactants [18,37,61], and for proteins [25,62–64] or foam stability against drainage [27]. However, in other studies no such correlation between the foam stability and interfacial properties was found [65–69]. For instance, the foam stability of whey, egg-white and algae protein stabilised foams increased significantly (i.e. for whey protein isolate the foam stability ($t_{5/6}$) increased from ~ 250 s to ~ 1500 s), while the elastic moduli were not significantly affected ($E_d \sim 70$ – 80 mN m $^{-1}$) [68]. Similar observations were reported in a study on the effect of pH on foam stability of β -lactoglobulin solutions [23], and for lysozyme heated to different extents [66,69]. The study by Braunschweig et al. on foams of β -lactoglobulin in presence of 0–1 M CaCl₂ [65] also showed that there were no correlations between foam stability (collapse or drainage) and either the viscous or elastic part of the surface dilatational modulus (Fig. 2).

In short, it is not evident from experimental data that the surface dilatational elasticity dominates, or explains, the foam stability. Of course, the values of the measured surface dilatational elasticity depend on the settings used for the measurement. It has been proposed that the lack between measured surface rheological parameters and foam stability is due to the fact that the timescales relevant during foam collapse are too different from those used during the measurements of the surface rheology [61,70]. In other words, the question is which deformation of the interface (amplitudes and frequencies) should be used in the experiment to obtain information relevant to the conditions in the collapsing foam. However, Noskov et al. also showed in several publications that the differences in surface dilatational elasticity were relatively independent of the frequency used [35,71,72]. Moreover, in the coalescence of bubbles in a foam, other factors may also play a significant role that are not as such reflected in the surface rheological properties. An example is the bubble size (distribution) that determines the pressure in the Plateau borders, and thereby the drainage rate (and equilibrium thickness) in the thin films. Especially when comparing results from different publications, but even within one study, variations in foam structure may influence the foam stability in a way that surface rheological properties are not dominant anymore.

1.5. Stability to coalescence of single bubbles and thin films: experimental evidence

To bridge the gap in length scales between the behaviour of a single air-water interface and foam stability, in some studies the stability of single bubbles or bubble rafts [15,73–75], or emulsion droplets [76] trapped under a planar surface was measured. In other studies, other properties of thin liquid films were measured, such as thickness, black spot formation, presence of aggregates [63,77,78]. Stubenrauch et al. studied the rupture stability of thin liquid films of low-molecular weight surfactants [79]. Based on that and earlier work, they stated that the rupture stability could not be solely explained based on the surface forces (disjoining pressure) in the film. They then continued to show a correlation between the stability of thin liquid films and the surface dilatational elasticity [79]. In contrast, Samanta et al. attributed the higher stability of thin liquid films of low-molecular weight surfactants (Brij, Tween) to the disjoining pressure [73,74]. Whether dominated by surface rheological properties or by disjoining pressure, a commonly used concept to describe stability of thin films is the Vrij criterion, described above. In this view, the thin films would rupture as soon as a certain critical thickness is reached. Some observations seem to show that this is not always the case. Langevin and Politova [80,81] showed

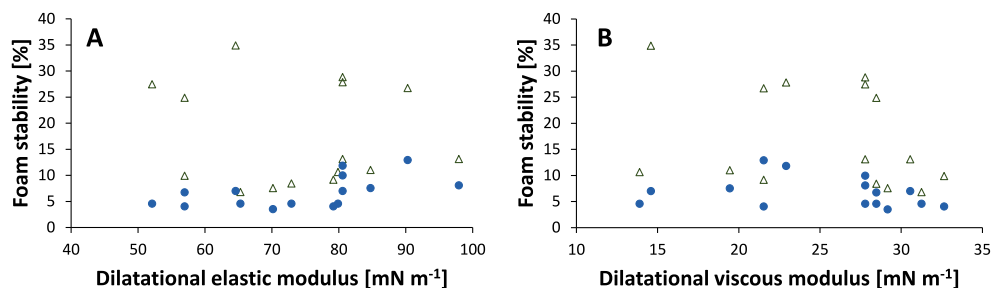


Fig. 2. Foam stability of β -lactoglobulin at pH \sim 6.7 in ultra-pure water with 0–1 M CaCl_2 versus the dilatational elastic (A) or viscous (B) modulus. Foam stability was expressed as the percentage decrease in height (Δ) or liquid volume measured by conductivity (\bullet) after 15 min relative to that at start of foam collapse ($t = 0$), based on [63].

that for some films the film lifetime was much larger than the drainage time. This shows that the films were stable for a definite amount of time at certain thickness before rupture (at that film thickness) occurred. A similar contradiction in literature was found for the effect of the film radius on the film stability. It has been suggested that the critical thickness of the thin film depends on its radius [31,53,82,83]. However, this seems to be contradicted by the results from Vakarelski et al. who showed examples where there was no strong correlation between the rupture time and film radius [84].

The above shows that there is still much to be understood on the relative contribution of the different mechanisms and parameters influencing thin film stability. The observed discrepancies between different studies may also, in part, be the consequence of some complicating factors in the understanding of thin film rupture. For low molecular weight surfactants, for example, the decrease of the thickness of the thin films occurs, under some conditions, in a stepwise fashion. This is also referred to as stratification, which is due to the confinement of micelles within the thin film [52,85–87]. For typical proteins, such behaviour is typically not observed, or at least it has not yet been described. In protein systems, on the other hand, aggregation can occur, especially when the sample has been heated or at a pH around the isoelectric point of the protein. Aggregates are typically visible as clear spots in the thin films [77,78]. To describe the possible effects of such aggregates on thin film stability, often links are made to the field of anti-foaming agents. The aggregates, or particles, that are trapped in the film can improve the stability, or induce rupture, depending on the number of particles, as well as their size, form and properties (e.g. hydrophobicity) [77,78]. Still, even for more homogeneous films, it seems that there are still many cases where the expected stability of thin liquid films, based on known interfacial and bulk properties does not match the experimental observations.

From the above, it may be clear that there is, still much to learn about which factors dominate the foam stability, and how this depends on conditions. In this study the stability of a set of similar (lager) beers was analysed. Several studies in the past have focussed on beer foam, for instance comparing the results from different foam tests [88,89]. Other studies focussed on identifying the differences in foam stability to the composition, or processing of the beer, i.e. presence of proteins and the hop iso α -acids [90–95]. In this work, a set of similar (lager) beers was analysed, using different foaming methods, as well as single bubble, thin liquid film and single interface methods. Based on the insights from all length scales, the aim was to evaluate the link between foam stability (against collapse) and interfacial properties.

2. New insights on foam stability

2.1. Foam stability and correlation with physicochemical properties

The foam stability of 24 lager beers, brewed according to similar recipes by various breweries, was analysed according to the NIBEM method. The foam stability of the beers ranged from around 206 s for the

beer with the least stable foam to 300 s for the beer with the most stable foam. Over the whole set, the foam stability followed a normal distribution (Fig. 3), which was expected since all lager beers were brewed according to similar recipes.

The variation in most physicochemical parameters (e.g. viscosity, pH, protein content) was relatively low, as expected for beers brewed to the same requirements (Table 1). No significant correlation was found between any of these measured parameters and the NIBEM foam stability, as reflected by the low values of the correlation coefficient (R^2) for linear fits.

Summarising, the compositional analysis and measurement of other properties (viscosity, pH) did not provide clear reasons for the observed differences in foam stability.

2.2. Effect of interfacial properties on foam stability

Based on literature, one would expect that the observed differences in foam stability would be reflected in difference in the interfacial properties. The increase of surface pressure in time, indicative of the adsorption kinetics, was similar for all samples on short- as well as longer timescales (i.e. 10 ms–3600 s; Fig. 4A and S1). The experiments on diluted samples (5% v/v) also showed no significant differences between the samples (data not shown). The interfacial dilatational modulus was increased from 5 to \sim 25 mN m $^{-1}$ for surface pressures between \sim 25–30 mN m $^{-1}$ (Fig. 4B). For all samples, the phase angle was on average $23 \pm 3^\circ$, and the real (elastic) part was $0.92 \times$ the complex modulus. The low surface modulus, as well as the shape of the E_d - Π curve is different from typical curves measured for pure protein systems [32–34,36,71]. The lower values for the surface dilatational modulus (at increased surface pressure) seems similar to the curves observed in mixed protein surfactant systems [36,96]. For the beer samples, the

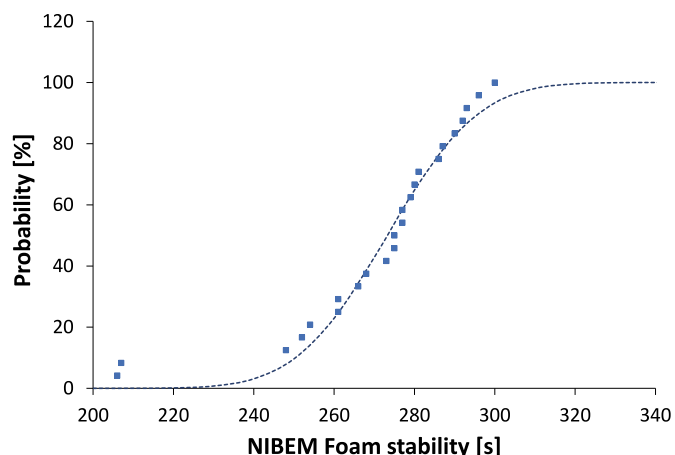


Fig. 3. Cumulative probability distribution of NIBEM foam stability for the beers in the total set, dotted line shows the fitted normal distribution curve.

Table 1

Range, minimum and maximum values for properties of the beer samples studied, as well as absolute and relative standard deviations (SD, RSD). None of these parameters had significant correlation (R^2) to the NIBEM foam stability (FS).

		Min	Max	Average	SD	RSD [%]	R^2 vs FS
Foam stability	[s]	206	300	270	24	8.9	
Original extract	[% w/w]	11.2	11.7	11.4	0.1	1.1	0.00
Real extract	[% w/w]	3.5	4.1	3.8	0.2	4.1	0.13
Apparent extract	[% w/w]	1.7	2.4	2.0	0.2	9.7	0.13
Specific gravity 20/20	[g mL ⁻¹]	1.0	1.0	1.0	0.001	0.1	0.13
Alcohol by volume	[% w/v]	4.6	5.2	5.0	0.12	2.5	0.13
CO ₂ (manometric method)	[% w/v]	0.5	0.6	0.5	0.02	4.6	0.18
Total isoalphacids	[mg kg ⁻¹]	18.7	26.4	21.9	1.8	8.2	0.50
Nitrogen	[mg kg ⁻¹]	611	835	700	52	7.5	0.05
Free amino nitrogen	[mg kg ⁻¹]	56	121	79	16	20.4	0.00
High molecular protein	[mg kg ⁻¹]	112	206	159	24	15.0	0.06
pH (degassed sample)	[–]	4.1	4.7	4.4	0.12	2.7	0.06
Viscosity at 20 °C	[mPa s]	1.5	1.7	1.6	0.06	3.8	0.10

dilatational properties may be a result of the hop iso- α -acids. The high similarity of interfacial properties of the different beer samples was also observed for the complex modulus versus surface pressure, the adsorbed amount in time, and the surface pressure during compression (Fig. 4C, D). In short, none of the interfacial properties showed any significant differences between the samples.

Additional experiments, such as the frequency dependence of the dilatational elastic modulus, and the surface shear elasticity all showed similar data for all samples (data not shown). Previously, Noskov et al. also showed the relative independence of differences in surface dilatational elasticity on the frequency [35,71,72]. Since no significant differences between the interfacial properties of different samples were observed, it was concluded that all classical explanations based on differences in adsorption kinetics, or elasticity of the interface could clearly not be used to explain the observed differences in foam stability. The next steps focussed on narrowing down the origin of the differences in foam stability from the macroscopic side.

2.3. Comparison of different foaming methods

It has been suggested that the method of producing the foam can have large effects on the foam stability [2]. It was therefore important to identify to which extent the ranking of samples on NIBEM foam stability depended on the method used. Therefore, other, alternative methods of foaming, such as sparging with N₂, and shaking were used to determine the foam stability and compare them with the NIBEM method. The ranking of the foam stability of different beers in these methods correlated with the ranking based on the NIBEM foam stability (Fig. 5).

The ranking was also retained when foaming with CO₂, or when measuring foam stability in dispensed beers (data not shown). This showed that the foam stability was dominated by intrinsic factors that were insensitive to the foaming method. Moreover, the similarity in ranking between foams made by CO₂ (NIBEM) and air/N₂ (shaking/

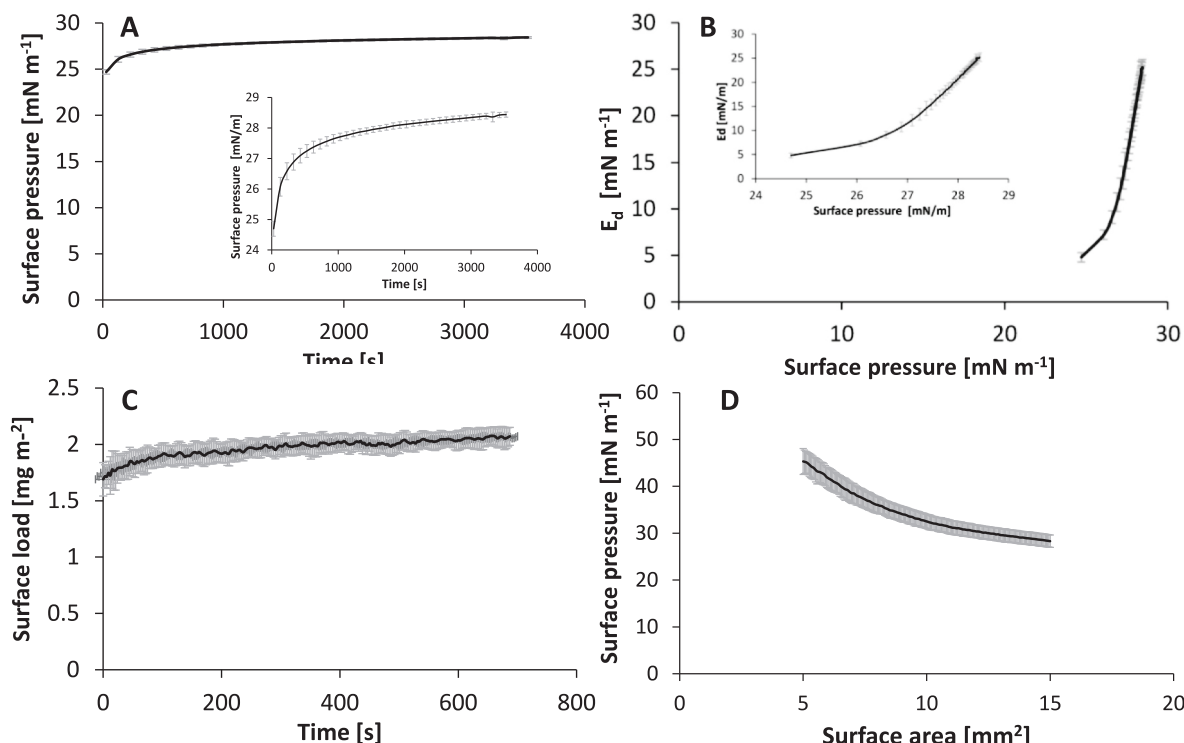


Fig. 4. Summary of interfacial properties determined for the beers, (A) surface pressure in time, (B) complex surface dilatational modulus as function of surface pressure, (C) surface load [mg m^{-2}] as measured by ellipsometry in time (beers with NIBEM foam stability of 207, 266 and 289 s, all measured in duplicate), and (D) the surface pressure versus surface area measured during compression of a single bubble in the PAT. Data in panel A, B and D were averaged over all beers (206–300 s NIBEM foam stability).

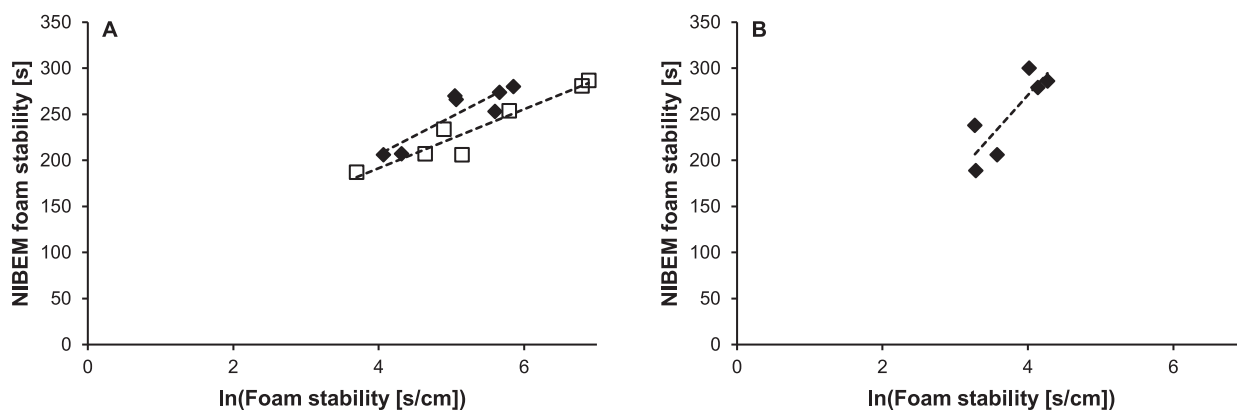


Fig. 5. Foam stability for different beers measured by the NIBEM method versus foam stability measured by other methods: (A) sparging test with N_2 with a 8 cm wide foam tube (\blacklozenge , $R^2 = 0.80$), and a 3.5 cm wide foam tube (\square , $R^2 = 0.92$) and (B) manual shake test with air ($R^2 = 0.72$).

sparging) with a significantly different solubility in water and therefore a significantly different rate of Ostwald ripening seems to indicate that the differences in foam stability between samples were dominated by coalescence, rather than Ostwald ripening (disproportionation).

2.4. Effect of particles on foam stability

Several studies have indicated the impact of particles on foam stability. For whey protein concentrates, for instance, the foam stability increased from 2.81 to 19 min after filtering (220 nm filter) the samples before the foam experiment [97]. In our study, filtration of the beer samples (using 100 and 200 nm filters) did not result in any measurable differences in foam stability (data not shown). Therefore, it was concluded that the observed differences in foam stability were, in this case, not caused by particles.

2.5. Foam stability is reflected in stability of single bubbles

Since the foam stability seemed to be dominated by coalescence, the next set of experiments determined the rupture time of (single) bubbles using the ‘bubble under the interface’ (BUI) method. In these experiments, no Ostwald ripening of the bubbles was observed before rupture of the film between the bubble and the air-water interface. Therefore, the observed differences in foam stability between the samples are considered to be due to differences in coalescence of the thin films, rather than differences in Ostwald ripening. This may also be relevant for other studies where the differences in foam stability between *similar*

samples is investigated, since there seems little evidence to suggest that in such sets Ostwald ripening would contribute significantly to the differences in foam stability. Before analysing and interpreting the rupture time, the bubble size distribution in different experiments was compared to evaluate the similarity between different experiments (Fig. 6). The bubble size distributions were similar between experiments (Fig. 6A). In addition, the data showed no clear correlation between bubble size and rupture time (Fig. 6B).

Only for some very small bubbles (typically <1 mm) a significantly higher rupture time was observed. This was not studied in detail, but assumed to be an effect of the lower force in the thin film, due to lower buoyancy force for smaller bubbles. These observations did not influence the conclusions, since most data collected was for bubbles with larger diameter, where no significant correlation was found with rupture time. Such a correlation was perhaps expected based on literature [39,82,98], but apparently in our experiment other factors were more dominant.

Clear differences are visible between the cumulative distributions of the single bubble rupture times for different samples (Fig. 7A). The average rupture time for each sample was determined by fitting Eq. (4) to the cumulative distributions of the rupture times. It should be noted that the absolute timescale of rupture of single bubbles are not identical to the timescale of coalescence in the foam (Fig. 7B). This is likely caused by differences in the size of the single bubbles and the bubbles in the foam, and therefore the forces acting on the thin film. Nevertheless, a very strong correlation between the average rupture time and NIBEM foam stability of different beers was obtained (Fig. 7B).

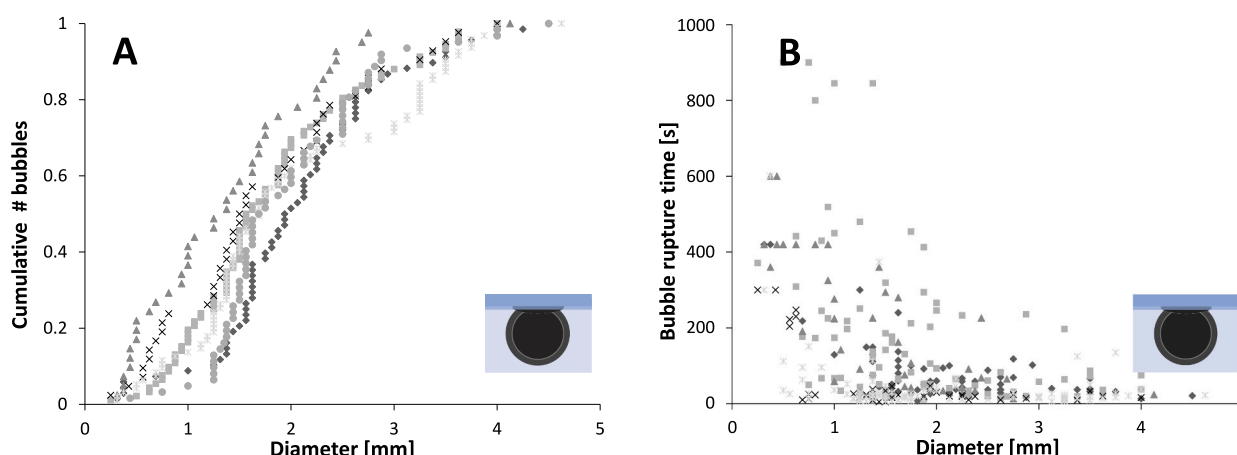


Fig. 6. (A) Typical cumulative distribution of bubble diameter for bubbles used to determine rupture times in ‘bubbles under the interface’ for several beers (206, 266, 270, 274, 280 and 287 s NIBEM foam stability), and (B) the rupture time versus diameter for the samples shown in panel A.

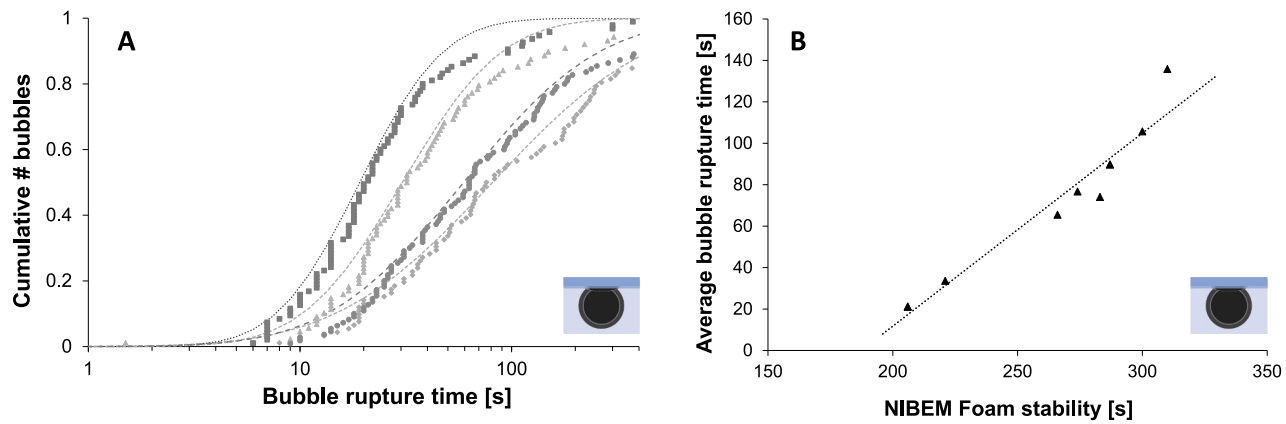


Fig. 7. (A) The cumulative rupture time distribution for single bubbles under the interface of different beers. Lines are from the fitted data, markers are experimental data for beers with NIBEM foam stability of ■-206, ▲-221, ●-266, ◆-287 s, (B) The average rupture time plotted against the NIBEM foam stability ($R^2 = 0.93$).

These data show that the intrinsic properties of the system that dominate the foam stability are retained in the coalescence stability of single bubbles under an air-water interface. This is highly important information, since this implies that the intrinsic foam stability, which in this case is coalescence driven, is reflected in the stability of the thin liquid films separating the single bubble from the bulk air-water interface. To investigate this in more detail, thin liquid films were studied.

2.6. Foam stability is reflected in stability of thin liquid films

The rupture times of thin liquid films of beer samples diluted at 1.5% v/v, were measured after different ageing times. Images of the thin films just before rupture show that the films of the different beers reach similar thicknesses (Fig. 8). The films were all quite homogeneous, i.e. there were no signs of aggregates in the thin films. Drainage typically started at the edge of the thin film, visible by the slightly darker colour at

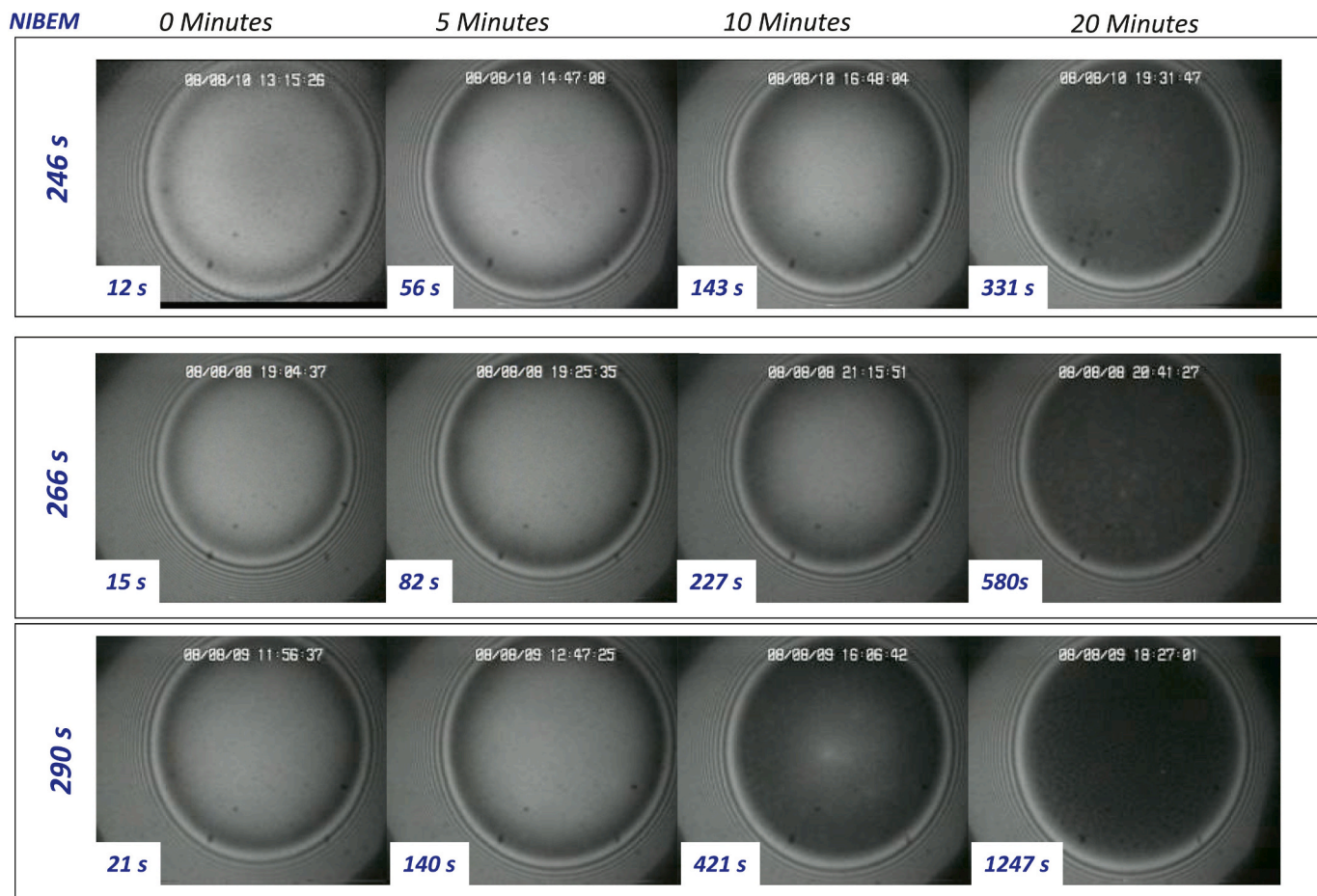


Fig. 8. Photos of thin liquid films (radii of around 100 μm) formed in the capillary cell for 1.5% v/v diluted beers with NIBEM foam stability of 246, 266 and 290 s. Films were made after different ageing times (0, 5, 10 or 20 min). Photos shown were those just before rupture occurred. Numbers shown in left bottom of photos are the rupture times of the films.

the edges. With increased ageing time, the films drain further, reaching lower (average) film thicknesses, until a homogenous thin film was reached, as shown for the films made after 20 min ageing (Fig. 8).

At short ageing time, the rupture times were very short, <50 s. With increasing ageing time, the rupture times increased dramatically (Fig. 9A). The stability of the thin liquid films was clearly higher for the beer samples with higher foam stability, even when taking into account the variation in the experimental data. This is reflected in the very strong correlation (R^2 0.95–0.99) between the thin film rupture time and the NIBEM foam stability (Fig. 9B). This difference in thin film stability was even more pronounced for samples aged for 20 min, where the rupture times range from ~300–1200 s for beers with NIBEM foam stability from 249 to 293 s respectively (Fig. 9B).

Apparently, even in a single thin film made with diluted samples, the rupture times still retained the intrinsic factors dominating foam stability. This shows that the underlying mechanisms dominating foam stability significantly affected the behaviour of these thin liquid films as well.

3. Understanding thin film rupture (and foam stability)

3.1. Contribution of thin film drainage

Since there were no significant differences in viscosity and interfacial properties of the samples (Table 1 and Fig. 4), the differences in foam, single bubble (Fig. 7) and thin film rupture times (Fig. 9) were expected to be due to differences in the drainage rate, equilibrium thickness, and/or disjoining pressure isotherms. Thin liquid film drainage was measured both in the closed and open capillary cell, so at high and low relative humidity respectively (Fig. 10), using non-diluted beer. In the closed capillary cell, the non-diluted beer samples showed initial thickness at opening of the film of 82 ± 8 nm (Fig. 10A). The films drained to reach equilibrium thickness of 30 ± 2 nm between 800 and 850 s after opening the film. For drainage in the open capillary cell, the drainage occurred faster, i.e. equilibrium thickness of 25 nm was reached after ~80 s (Fig. 10B). For these films, the contact angle of different samples was calculated to be similar $\sim 1 \pm 0.5^\circ$. In the open cell, the thickness versus times curves were similar for all samples, showing that the drainage rates for all samples were similar. Nevertheless, the rupture in open cell occurred at shorter times (63 ± 40 s) for the beer with a low stability than for the beer with a high foam stability (129 ± 24 s).

In summary, all samples showed similar drainage rates and equilibrium thicknesses. In basis, this was expected, since the most relevant properties, the interfacial properties as well as the bulk viscosities, of all samples were similar. These results however posed a problem, as the

drainage rate and equilibrium thickness did not provide any reason to explain the differences in the observed stability of the films against rupture. Moreover, the observed difference in thin film stability at similar equilibrium thickness is in contrast with typical theoretical descriptions of thin film stability provided in literature. Based on the Vrij criterion, it is assumed that films will rupture (instantaneously) at the moment that a certain critical film thickness is reached [39,45,82,98]. In this view, the rupture time will be determined by the time needed to reach this critical thickness, i.e. the drainage rate. Therefore, it was expected that samples with lower film stability would either drain faster (to reach the critical film thickness), or rupture at larger film thickness, which was not observed in the thin film data. Similar observations were reported by Szekrényes et al. who also showed that thin films, between a single bubble under a planar surface, did not rupture instantaneously after reaching the minimal thickness, but after being at the minimal thickness for a certain amount of time [75].

3.2. Contribution of disjoining pressure

To provide somewhat more insight into the forces at work in the thin liquid films, the disjoining pressure isotherms were measured in the porous cell (Mysels cell). The thin films of all diluted beer samples drained to an equilibrium thickness of around 40 nm, at a pressure of ~120 Pa (Fig. 11). For all samples, an increase to ~300 Pa resulted in a decrease of film thickness to ~30 nm. The films formed with samples with low foam stability already ruptured at pressures between 200 and 400 Pa. For the samples with the highest foam stability (NIBEM foam stability of 280–293 s), the pressure could be increased up to 2000 Pa, resulting in a film thickness of ~20 nm. The similarity in the disjoining pressure isotherms for the different samples (except the pressure and thickness at rupture) indicates that the electrostatic and steric repulsive forces in the thin films were similar for all samples. This again agrees with the observation that the interfacial properties and pH, ionic strength etc. were similar for all samples.

3.3. Contribution of the liquid between the interfaces

As discussed above, the foam stability of the individual samples was reflected in different foam experiments, the stability of single bubbles under the interface, as well as the stability of thin liquid films. At the same time, the samples appeared all essentially identical when considering the viscosity, the single interface properties as well as the drainage rate, equilibrium film thickness and disjoining pressure isotherms. This posed a serious question as to the applicability of the current state of knowledge on foam stability. Based on the current consensus in literature, any set of samples where all these properties are similar (if not

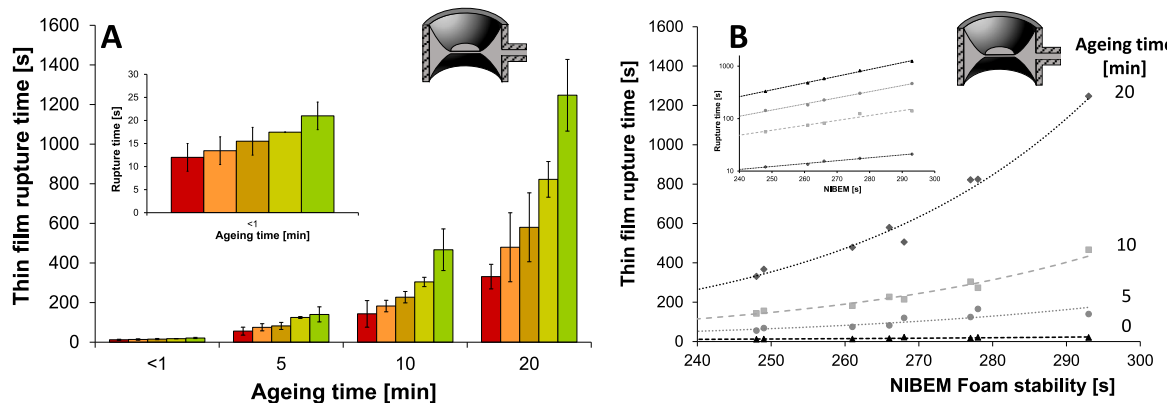


Fig. 9. (A) Typical rupture times of thin liquid films (in closed capillary cell) determined after 0–20 min ageing for 1.5% v/v diluted beers with original NIBEM foam stability of 248, 261, 266, 277, 290 s (from left to right). Inset in panel A shows the rupture times without ageing (i.e. ageing time = 0 min), (B) rupture times plotted versus the NIBEM foam stability (lines indicate exponential trendlines R^2 : 0.95–0.99). Inset in panel B shows same data but with logarithmic Y-scale.

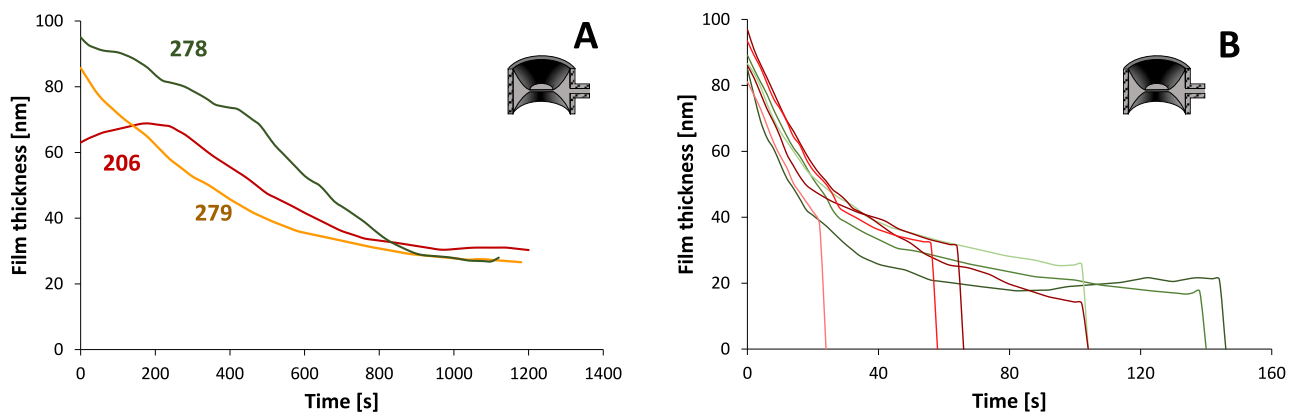


Fig. 10. Drainage in thin liquid films in a closed (A) and open (B) capillary cell for non-diluted beer with NIBEM foam stability of (A, B) 206, 278 and (A) 279 s.

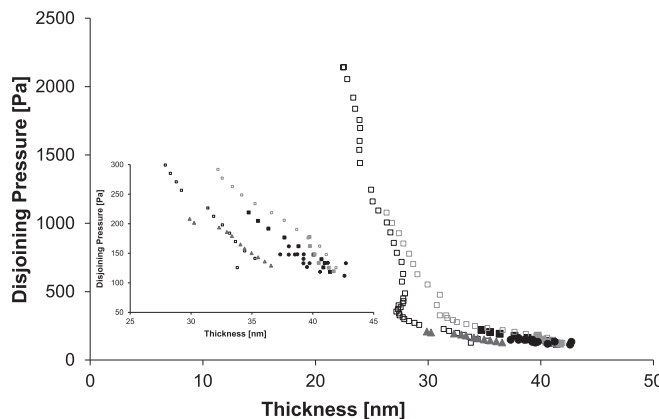


Fig. 11. Disjoining pressure isotherm for 1.5% v/v diluted beer samples (NIBEM foam stability of 287 s aged for 8-■, 15-■, and 20-□ and 30-□ minutes) and NIBEM foam stability of 207 s-fresh and after ageing (◆, ◆) and 266 s-▲. Note that samples with low foam stability ruptured at pressures <400 Pa (see inset).

identical) should have the same foam stability. Similarly, for the thin films the rupture times would be expected to be similar given the fact that all measured properties were similar. The only thing that perhaps was not taken into account, was the composition of the liquid in between the air-water interfaces in the thin liquid films. This liquid was not identical for the different samples, even though there were no significant differences in viscosity or composition. The influence of this liquid was tested using a modified capillary cell [99]. The benefit of this modified cell is that it allows the exchange of the bulk liquid in between the two air-water interfaces. To test the effect of exchange of bulk liquid on the surface pressure, experiments were performed in the PAT where the liquid in a droplet was exchanged to buffer (Fig. 12). For a pure hop solution, the surfactants adsorbed at the interface clearly desorbed from the interface when the exchange started. This is typical behaviour also shown for other low molecular weight surfactants [99–102]. For the beer samples, where proteins (perhaps in non-covalent association to hop components) were adsorbed to the interface, no change in surface pressure was detected. This is in line with other studies on pure proteins, where for globular proteins typically no desorption was observed under these conditions [100]. These observations indicate that exchanging the bulk liquid does not affect the adsorbed protein layer.

Next, the effect of bulk exchange on the rupture time of thin films was studied in the modified capillary cell. The films after exchange with buffer always had relatively low film stability (Fig. 13). However, even after exchange of buffer the film stability increased with increasing ageing time. This is attributed to the formation of the adsorbed layer. At

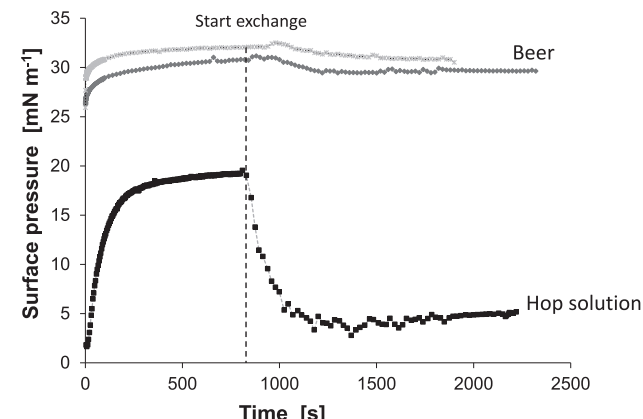


Fig. 12. Surface pressure as function of time for a solution of (■) hop and beer (NIBEM foam stability of 254-◆, and 207 *) samples before and after exchange of the bulk liquid with Na-acetate buffer with 5% ethanol.

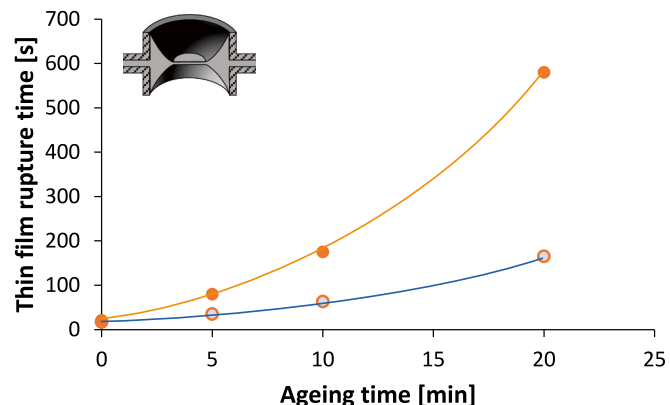


Fig. 13. Thin film rupture times for beer with NIBEM foam stability of 266 s before (●) and after (○) exchange of liquid in the film with buffer at different ageing times of the adsorbed layers.

each ageing time, the film without exchange of liquid in the film has a higher film stability. The difference in thin film stability for the films as is and after exchange increased with ageing time. After 20 min ageing time the exchange of the liquid in the bulk by buffer resulted in a significantly lower rupture times, i.e. rupture time decreased from ~580 to 165 s (Fig. 13).

For three beers, after ageing the interfaces for 20 min, the bulk liquid was replaced by buffer. After this exchange, the rupture time was the

same for all samples, i.e. ~ 200 s (Fig. 14A). This was in a way expected, since the interfacial properties were known to be the same and the thin films were made from 'identical' interfacial layers and -after exchanging the same liquid (buffer) in the middle of the film. At the same time, it indicates that the liquid between the interfaces has a large effect on the film stability. It is important to remember that this effect cannot be explained by differences in viscosity (Table 1), nor by the effect of larger particles (i.e. no effect of filtration). In literature, the existence of weakly adsorbed multilayers has been suggested, the presence of which is not reflected in a change in surface pressure or other measurements. In that view, the exchange of bulk liquid is often thought to result in a change of the adsorbed layer from a multilayer prior to exchange to a monolayer after exchange. Since multilayer formation was suggested to (potentially) enhance foam stability [103–105], this may be a possible reason for the observed difference in thin film (and foam) stability resulting from bulk liquid exchange. Since the interfacial and thin film properties (such as drainage rate and disjoining pressure isotherms) were similar for all beers and more importantly the equilibrium surface load of all beers was ~ 2 mg/m² (i.e. corresponding to the adsorbed amount for a monolayer) [106,107], multilayer formation can be excluded as possible explanation for the observed differences caused by bulk liquid exchange.

To verify the effect of the liquid between the films, another set of experiments was performed where for each sample the liquid in the film was exchanged with another sample solution instead of buffer (Fig. 14B). In all cases, the rupture times of the samples after exchange became similar to that of the sample used for the exchange. To be specific, the rupture time of samples with low original stability was significantly increased when the exchanged with a solution from a sample with high stability, and vice versa. The effect was consistently measured for samples from both batches (from two different years). At this moment, there is no clear indication which factor or property in these samples results in the different stability against rupture.

4. Conclusions and future outlook

Differences in foam stability are typically considered to be directly related to differences in drainage, Ostwald ripening or coalescence. Differences in these mechanisms are then attributed to differences in interfacial (e.g. surface rheology) and bulk properties (e.g. viscosity). Using a range of experiments on macroscopic (foam) and lower length scales (single bubbles, thin liquid films) it was shown that the differences in foam stability were reflected in the stability of the thin liquid films. In other words, the differences in foam stability were dominated by intrinsic differences in stability against coalescence of the thin films, and not by drainage, initial bubble size distribution, or Ostwald ripening. For the samples used in this study, the large variation in foam (and

coalescence) stability could not be explained by variations in the properties of thin liquid films, or single interfaces, as is typically described in literature. To screen for differences in foam stability it may therefore be more relevant to study the rupture of single bubbles under the interface than the properties of single interface. The observed differences in stability against coalescence, as mentioned, was not linked to differences in any of the conventional parameters measured. There was, however, a clear and significant contribution from the solution in between the adsorbed layers of a thin film on the thin film stability. By exchanging this solution, we were able to illustrate the importance of this liquid to the rupture stability of thin films. At this moment, it remains difficult to pose a coherent hypothesis to explain these observations based on the current theoretical descriptions of factors and mechanisms determining foam stability. This illustrates the need to review our current understanding of coalescence phenomena and to develop new methods both in experimental study and theoretical description of such systems.

5. Methods

5.1. Materials

Three sets of lager beer samples, from breweries from all over the world were used. From each brewery one lager beer (per year) was sampled, and all samples were brewed with similar recipes. The first set consisted of beers from 6 breweries, the second set of beers was collected a year later from 7 breweries. Again, a year later beers from 11 breweries were collected, including 2 which showed minimal and maximal foam stability in previous experiments which were used for more detailed studies.

5.2. Chemical characterization

The beers were analysed using typical methods (<https://brewup.eu/ebc-analytica/>) to determine the original extract, real extract, alcohol and gas contents as well as total content of isoalpha-acids, total protein (using Kjeldahl, N*6.25), free amino nitrogen using the ninhydrin method, and high molecular weight using the Bradford assay (see e.g. [108]).

5.3. Viscosity

The viscosity was measured with an Ubbelohde (PSL_Rheotek, Essex, UK). The flow time through the capillary was measured, and the kinematic viscosity was calculated using Eq. (3). The density was measured with an DMA 5000 density meter (Anton Paar, Graz, Austria). Each sample was measured at a temperature of 5 °C. The viscosity as well as

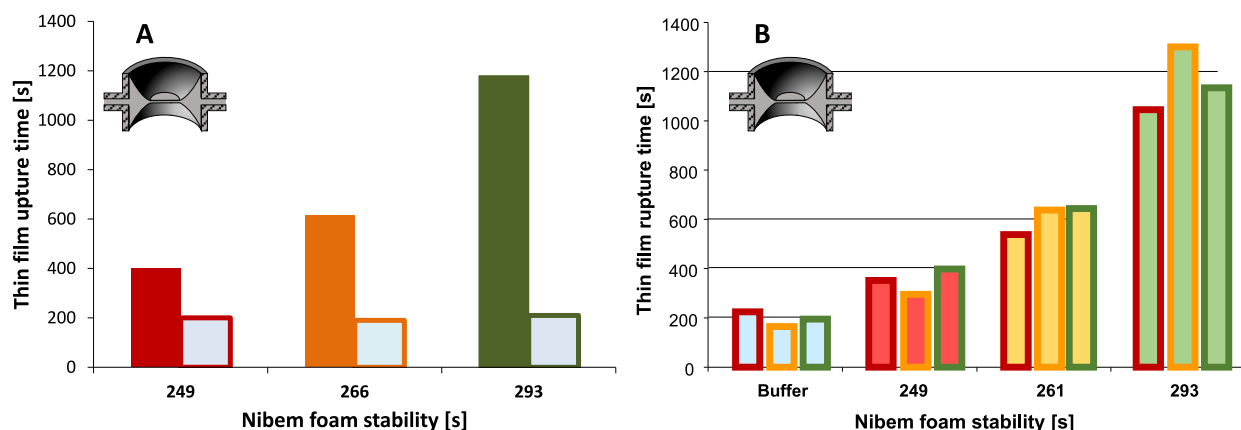


Fig. 14. Rupture times before and after exchange of the bulk liquid -all after 20 min ageing time, (A) for three 1.5% v/v diluted beers (NIBEM foam stability of 249, 266, and 293 s) before and after exchange of liquid by buffer, and (B) for three samples before and after exchange with either buffer, or one of the other samples. In each bar, the outline colour indicates first sample to be placed in the exchange cell, the fill colour indicates the sample used for the exchange.

density were measured in duplicate.

$$\eta = 10^{-6} \bullet C \bullet t \bullet \rho \quad (3)$$

Where η is the dynamic viscosity [Pa s], C is the cell constant at 25 °C [0.004639 mm² s⁻²], t is the flow time [s], and ρ is the density [kg m⁻³].

5.4. Preparation of degassed beer

Beer was degassed by slowly pouring it into a beaker to avoid and minimise foam formation. After the initial excess of gas was removed, the sample was stirred very slowly using a magnetic stirrer for at least 2 h at room temperature. After this treatment, no nucleation was observed in the solution.

5.5. Foam stability

NIBEM: The beer foam stability was measured using the NIBEM, FST Foam Stability Tester (FST-100TPH, Haffmans BV, Venlo, the Netherlands). Beer was transferred from the bottle to the standard glass cup using the ISD-3000 sampling device, followed by injection of compressed CO₂. The glass cup containing the foam was then placed in the NIBEM measuring device with electrodes positioned at the top of the foam. When the foam had collapsed to a pre-set distance of 10 mm below the reference position, time recording automatically began. Upon foam collapse, the electrode system kept moving downward until the foam had collapsed another 30 mm, to reach 40 mm below the reference position. The NIBEM foam stability, was expressed as the time needed for the foam to collapse over this distance.

Shaking: The degassed beer (10 mL) was placed into a 100 mL cylinder which was subsequently closed and shaken by hand intensively for 1 min. The cylinder was then opened, and the foam and liquid height were monitored in time.

Sparging (with CO₂ or N₂): The degassed beer was placed into a sparging cylinder (radius 3.1 cm, height 13 cm) [69]. For each measurement fresh solution (60 mL) was placed in the beaker, and N₂ or CO₂ was sparged through a metal frit into the solution at a flow rate of around 100 mL min⁻¹, until the foam height reached 12 cm. After the gas flow was stopped, the foam height was recorded as a function of time. To correct for minor differences in initial foam height, the relative foam height was calculated by dividing foam height at $t = x$ by the foam height at $t = 0$. All samples were measured at least in duplicate. For this experiment, also tests were performed using beer samples after filtering over a 100 nm or a 200 nm filter.

Foam stability: For the NIBEM method, the time taken for foam decay from 10 to 40 mm was taken as measure of foam stability. For both the shake test and the sparging experiment, the inverse slope of the foam height versus time (in s cm⁻¹) was used as indication of the foam stability.

5.6. Bubbles under the interface

The stability of bubbles against coalescence (film rupture) was determined using the setup previously applied for emulsion droplets [76], and similar to other described methods [15,73,74]. A glass ring was placed in a wide beaker with a larger diameter that contained the sample solution (Fig. 15). The glass ring was used to support a Teflon plate with two holes. Degassed beer was poured in the vessel until there was a curved meniscus in the hole of the Teflon plate. Through one of the holes a glass Pasteur pipette was placed in such a way that the tip was below the other hole (Fig. 15). Then, a single or small number (<5) of bubble(s) was released from the pipette tip. In our experiments, the bubbles all disappeared after some time due to rupture of the thin liquid film between the bubble and the air-water interface of the bulk liquid. In other words, no coalescence between the bubbles and no disappearance of bubbles due to Ostwald ripening was observed.

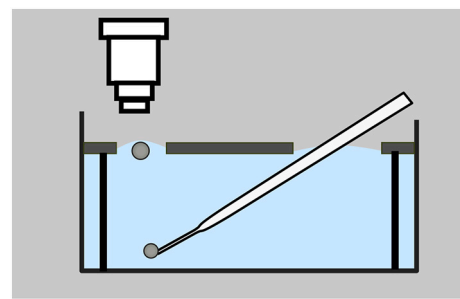


Fig. 15. Schematic illustration of the set-up used for the determination of the lifetime of single bubbles under the interface.

Images were recorded by video, in order to later extract the size as well as the average lifetime of the bubbles (t_R [s]), i.e. the rupture time. Data were collected to have at least >100 bubbles recorded for each sample. A lognormal cumulative distribution function (Eq. (4)) was used to fit the experimental data (with minimizing on the sum of squared errors).

$$P(t) = 1 / LN(t_R) * \sqrt{2\pi} * e^{(-LN(t-t_R)^2 / (2t_R^2))} \quad (4)$$

Where $P(t)$ is the probability of rupture, or the cumulative number of bubbles rupture at time t . The average rupture time (t_R) of the bubbles under the interface obtained in this way was reproducible to <10% between experiments. Fitting rupture times with a stochastic function was previously also done for rupture times of bubbles, e.g. [74,109–111], and of thin liquid films [82].

5.7. Single interface properties

Bubble pressure analysis (BPA): The surface pressure was measured on short-time scales (10–10,000 ms) using the BP-100 (Krüss, Hamburg, Germany).

Automated drop tensiometry (ADT): The surface pressure and viscoelastic modulus were measured as function of time (0–3600 s) using the automated drop tensiometer (Tracker, ITConcept, France) as described by Wierenga et al. [112]. For each experiment, a new air bubble (5 μ L) was formed in the degassed beer. Measurements were performed at 20 °C in duplicate. Since the change in surface pressure was relatively fast in the degassed beer, experiments were also performed with samples diluted to 5% (v/v) in demi water. The dilatational rheological properties were measured using a deformation of the bubble area with 5% at a frequency of 0.1 Hz. In separate experiments, an amplitude sweep from 5 to 20% of the bubble area was applied.

Compression experiments: To study the effect of large-scale compression of the interface, additional experiments were performed with degassed beer. After bubble formation at an initial volume of 5 μ L, the proteins were allowed to adsorb for 1200 s. Next, the bubble volume was slowly decreased to ~0.5 μ L.

Bulk exchange experiments: A double-capillary setup in the profile analysis tensiometer (PAT, Sinterface, Berlin, Germany) was used to measure the effect of exchanging the bulk liquid [113]. First a droplet of 5 μ L was formed with the degassed beer. After 1200 s, the bulk exchange was started by simultaneously pumping buffer (10 mM Na-acetate buffer pH 4.5 containing 5% ethanol) into the droplet through the inner capillary and removing liquid from the droplet through the outer capillary.

Ellipsometry: A combined setup of a multi-skop ellipsometer (Optrell, Germany) and Langmuir trough (Riegler and Kirstein, Germany) was used, as described earlier [112]. The angle of incidence was 50°. For the samples, the values of the refractive indices of air (1.0) and protein solution (1.3327) as well as the refractive index increment ($dn/dc = 0.18$) [114,115] were used. For a clean air-water interface the

measured values were $\Delta = 180.128^\circ$ and $\Psi = 5.080^\circ$.

Surface shear: The surface shear modulus measured using a rheometer (Anton Paar MCR 301) was measured as described by Philipp Erni et al. [116]. A stainless steel biconical disc was coupled to the disc holder attached to the top driven motor and the torque and normal force were monitored. The disc was placed into the air/water interface such that the disc edge was in the plane of the air/water interface. Each solution was measured by starting with a time sweep; constant strain 1% and constant frequency 1 Hz, followed by a frequency sweep; constant strain 1% and a frequency changing logarithmic from 0.01 to 5 Hz and finally, a strain sweep; constant frequency 1 Hz and a strain changing logarithmic from 0.1 to 100%. The surface shear was determined over time, with each different sweep taking 10 min. The temperature was kept constant at 20 °C or 5 °C with a temperature-controlled measurement cell.

5.8. Thin liquid film properties

5.8.1. Capillary cell

The thin films formed in the capillary cell (capillary pressure is 40–50 Pa) were observed under reflected light ($\lambda = 546$ nm), using the setup described previously [54,58,69,117,118]. The intensity of the reflected light was used to calculate the film thickness (as described previously [119]). Additional information on the technique and obtained results were reported in detail by others [50,120,121].

Experiments were performed in both the open and closed cell configuration. In the closed cell experiments, around 5 mL of liquid was placed in the bottom of the cell holder and a glass was placed on top of the cell holder. Under these conditions, evaporation of liquid from the thin film was prevented, or at least significantly reduced. Drainage rates were determined for films from undiluted beer made without dimples. Rupture times were measured in diluted samples, since the rupture times exceeded 1800 s for all non-diluted samples.

The conditions of the experiments to determine rupture times were optimized in order to have rupture times within practical timescales. Therefore, in a first pre-screening set of experiments the ageing time (time that the protein solution was in the cell prior to the formation of a film) and the concentration of beer in the solution were varied (0–20 min and from 0.1 to 5% v/v). Based on these results, it was decided to use the diluted degassed beer diluted to 1.5% v/v with 10 mM Na-acetate at pH 4.5, and to make films after 20 min adsorption/equilibration in the thin film cell. After this ageing time, a thin film (radius ~ 100 μm) was formed without dimple. The rupture times of the films (up to 1800 s) were registered. For each sample at least 50 films were measured. The data were used to plot the cumulative lifetime distribution, from which the average lifetime (rupture time) of the thin film for each sample was determined, similar as described for the single bubbles under a planar interface.

5.8.2. Capillary exchange cell

In the capillary exchange cell, the solution between the two adsorbed layers can be exchanged for a second solution, as described previously [99]. This set-up was used to determine the effect of the non-adsorbed molecules from the bulk solution on thin film behaviour. The dimensions of the cell and capillary were similar as for the normal capillary cell, and for these experiments the beers were also diluted to 1.5% v/v with 10 mM Na-acetate at pH 4.5. For each analysis, a series of steps had to be taken (Fig. 16). First, a small volume of liquid 1 (the buffer that was also used for dilution) was sucked into one capillary (i.e. side-capillary A). Subsequently, a small volume of liquid 2 was inserted into the capillary cell. Molecules from liquid 2 were allowed to adsorb to the air-water interface for a certain amount of time (0–20 min). Afterwards, the liquid between the two air-water interfaces was replaced by liquid 1 by sucking liquid 2 from the capillary cell into side-capillary B, while pushing additional liquid 1 into the capillary cell from side-capillary A. The film holder had an internal diameter of 2.6 mm and

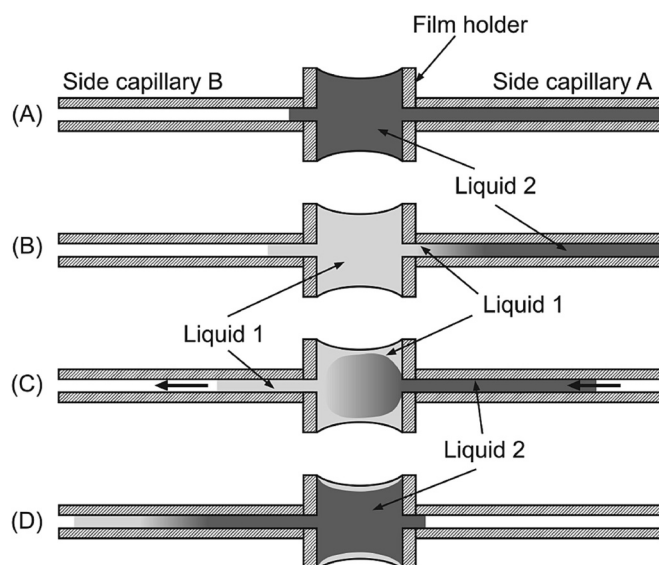


Fig. 16. Illustration of the exchange of the liquid in the double capillary cell, from: [108]. (A) Step 1: filling of the film holder and one of the side capillaries (denoted as capillary A) with liquid 2. (B) Step 2: rinsing of the film holder with liquid 1 (using an external pipet), where a small amount of liquid 1 is sucked into side capillary A. (C, D) Step 3: exchange of liquid 1 in the film holder with liquid 2 while maintaining the adsorption layers formed during step 2.

height of 3 mm. The two attached side capillaries had an internal diameter of 0.8 mm and a length of 25 cm. The liquid volume in the side capillaries was around 400 μL , which is approximately 10 times the volume of the liquid contained in the film holder (i.e. 40 μL). Typically, the time taken to complete the exchange of bulk liquid was ~ 1 –2 min. It was previously shown using SDS solutions [122] that this approach indeed allowed an efficient exchange of liquid between the adsorbed layers at the air-water interfaces.

5.8.3. Porous cell

The porous cell used, or: thin film pressure balance, was coupled to a pressure sensor and a capillary. A syringe connected to the capillary was used to adjust the pressure in the films, as described previously [122]. This setup was described first by Mysels and Jones [123] and later by Dimitrova et al. [58]. As in the capillary cell experiments, the thickness of the film was measured from the intensity of reflected light. By simultaneous measurement of pressure in and the thickness of the film, the disjoining pressure isotherm was constructed. It may be clear that once the solution is placed in the film holder, adsorption starts. To assure that all experiments were performed under similar condition, the time between placement of solution and start of the measurement was taken to be around 20 min (similar as for capillary cell experiments).

Funding information

This research was funded by Heineken Global Supply Chain BV, Zoeterwoude, The Netherlands as part of the SenterNovem FOAMS project.

CRedit authorship contribution statement

Peter Alexander Wierenga: Conceptualization, Methodology, Validation, Formal analysis, Investigation, Writing – original draft, Writing – review & editing, Visualization. **Elke Simeonova Basheva:** Methodology, Formal analysis, Investigation, Writing – original draft, Writing – review & editing. **Roy Jozef Bernard Marie Delahaije:** Validation, Writing – review & editing.

Declaration of Competing Interest

The authors declare no known competing financial interests nor personal relationships that could have influenced the work.

Data availability

Data will be made available on request.

Acknowledgments

We would like to thank Nikolai Denkov and Marcel Meinders for the fruitful discussions.

Appendix A. Supplementary data

Supplementary data to this article can be found online at <https://doi.org/10.1016/j.cis.2023.102845>.

References

- [1] Bhakta A, Ruckenstein E. Decay of standing foams: drainage, coalescence and collapse. *Adv Colloid Interface Sci* 1997;70:1. [https://doi.org/10.1016/s0001-8686\(97\)00031-6](https://doi.org/10.1016/s0001-8686(97)00031-6).
- [2] Hailing PJ, Walstra P. Protein-stabilized foams and emulsions. *Crit Rev Food Sci Nutr* 1981;15:155. <https://doi.org/10.1080/10408398109527315>.
- [3] Langevin D. Influence of interfacial rheology on foam and emulsion properties. *Adv Colloid Interface Sci* 2000;88:209. [https://doi.org/10.1016/S0001-8686\(00\)00045-2](https://doi.org/10.1016/S0001-8686(00)00045-2).
- [4] Maldonado-Valderrama J, Martín-Molina A, Martín-Rodríguez A, Cabrerizo-Vilchez MA, Gálvez-Ruiz MJ, Langevin D. Surface properties and foam stability of protein/surfactant mixtures: theory and experiment. *J Phys Chem C* 2007;111:2715. <https://doi.org/10.1021/jp067001j>.
- [5] Meinders MBJ, Van Der Smar RGM. Modeling foam stability. In: *Computational methods for complex liquid-fluid interfaces*. 503; 2015.
- [6] Narsimhan G, Xiang N. Role of proteins on formation, drainage, and stability of liquid food foams. *Annu Rev Food Sci Technol* 2018;9:45. <https://doi.org/10.1146/annurev-food-030216-030009>.
- [7] Panizzolo LA, Mussio LE, Anón MC. A kinetic description for the destabilization process of protein foams. *Int J Food Prop* 2012;15:60. <https://doi.org/10.1080/10942911003687264>.
- [8] Rodríguez Patino JM, Carrera Sánchez C, Rodríguez Niño MR. Implications of interfacial characteristics of food foaming agents in foam formulations. *Adv Colloid Interface Sci* 2008;140:95. <https://doi.org/10.1016/j.cis.2007.12.007>.
- [9] Wasan DT, Nikolov AD, Lobo LA, Koczo K, Edwards DA. Foams, Thin Films and surface rheological properties. *Prog Surf Sci* 1992;39:119. [https://doi.org/10.1016/0079-6816\(92\)90021-9](https://doi.org/10.1016/0079-6816(92)90021-9).
- [10] Rodríguez Patino JM, Minones Conde J, Linares HM, Pedroche Jiménez JJ, Carrera Sánchez C, Pizones V, et al. Interfacial and foaming properties of enzyme-induced hydrolysis of sunflower protein isolate. *Food Hydrocoll* 2007;21:782. <https://doi.org/10.1016/j.foodhyd.2006.09.002>.
- [11] Tamm F, Sauer G, Scampicchio M, Drusch S. Pendant drop Tensiometry for the evaluation of the foaming properties of Milk-derived proteins. *Food Hydrocoll* 2012;27:371. <https://doi.org/10.1016/j.foodhyd.2011.10.013>.
- [12] Zhang H, Xu G, Liu T, Xu L, Zhou Y. Foam and interfacial properties of tween 20-bovine serum albumin systems. *Colloids Surf A Physicochem Eng Asp* 2013;416:23. <https://doi.org/10.1016/j.colsurfa.2012.10.028>.
- [13] Wang J, Nguyen AV, Farrokhpay S. A critical review of the growth, drainage and collapse of foams. *Adv Colloid Interface Sci* 2016;228:55. <https://doi.org/10.1016/j.cis.2015.11.009>.
- [14] Gochev GG, Ulaganathan V, Retzlaff I, Gehin-Delval C, Gunes DZ, Leser M, et al. β -Lactoglobulin adsorption layers at the water/air surface: 4. Impact on the stability of foam Films and foams. *Minerals* 2020;10:1. <https://doi.org/10.3390/min10070636>.
- [15] Chandran Suja V, Rodríguez-Hakim M, Tajuelo J, Fuller GG. Single bubble and drop techniques for characterizing foams and emulsions. *Adv Colloid Interface Sci* 2020;286. <https://doi.org/10.1016/j.cis.2020.102295>.
- [16] Audebert A, Saint-Jalmes A, Beaufils S, Lechevalier V, Le Floch-Foutré C, Cox S, et al. Interfacial properties, film dynamics and bulk rheology: a multi-scale approach to dairy protein foams. *J Colloid Interface Sci* 2019;542:222. <https://doi.org/10.1016/j.jcis.2019.02.006>.
- [17] Chen S, Zhou Y, Wang G, Li W, Zhu Y, Zhang J. Influence of foam apparent viscosity and viscoelasticity of liquid Films on foam stability. *J Dispers Sci Technol* 2016;37:479. <https://doi.org/10.1080/01932691.2015.1045599>.
- [18] Aono K, Suzuki F, Yomogida Y, Okano T, Kado S, Nakahara Y, et al. Relationship between air-water interfacial Dilational viscoelasticity and foam property in aqueous solutions of sodium Alkylsulfates with different hydrocarbon chains. *J Dispers Sci Technol* 2021;42:1218. <https://doi.org/10.1080/01932691.2020.1731529>.
- [19] Buzzacchi M, Schmiedel P, Von Rybinski W. Dynamic surface tension of surfactant systems and its relation to foam formation and liquid film drainage on solid surfaces. *Colloids Surf A Physicochem Eng Asp* 2006;273:47. <https://doi.org/10.1016/j.colsurfa.2005.06.074>.
- [20] Dombrowski J, Mattejat C, Kulozik U. Correlation between surface activity and foaming properties of individual Milk proteins in dependence of solvent composition. *Int Dairy J* 2016;61:166. <https://doi.org/10.1016/j.idairyj.2016.05.006>.
- [21] Britten M, Lavoie L. Foaming properties of proteins as affected by concentration. *J Food Sci* 1992;57:1219. <https://doi.org/10.1111/j.1365-2621.1992.tb11303.x>.
- [22] Delahajie RJBM, Lech FJ, Wierenga PA. Investigating the effect of temperature on the formation and stabilization of ovalbumin foams. *Food Hydrocoll* 2019;91:263. <https://doi.org/10.1016/j.foodhyd.2019.01.030>.
- [23] Lech FJ, Delahajie RJBM, Meinders MBJ, Gruppen H, Wierenga PA. Identification of critical concentrations determining foam ability and stability of β -Lactoglobulin. *Food Hydrocoll* 2016;57:46. <https://doi.org/10.1016/j.foodhyd.2016.01.005>.
- [24] Marinova KG, Basheva ES, Nenova B, Temelska M, Mirarefi AY, Campbell B, et al. Physico-chemical factors controlling the Foamability and foam stability of Milk proteins: sodium Caseinate and whey protein concentrates. *Food Hydrocoll* 1864;2009:23. <https://doi.org/10.1016/j.foodhyd.2009.03.003>.
- [25] Martin AH, Grolle K, Bos MA, Cohen Stuart MA, Van Vliet T. Network forming properties of various proteins adsorbed at the air/water Interface in relation to foam stability. *J Colloid Interface Sci* 2002;254:175. <https://doi.org/10.1006/jcis.2002.8592>.
- [26] Medrano A, Abirached C, Araujo AC, Panizzolo LA, Moyna P, Añón MC. Correlation of average hydrophobicity, water/air Interface surface rheological properties and foaming properties of proteins. *Food Sci Technol Int* 2012;18:187. <https://doi.org/10.1177/1082013211415137>.
- [27] Ruiz-Henestrosa VP, Sánchez CC, Escobar MDMY, Jiménez JJP, Rodríguez FM, Patino JMR. Interfacial and foaming characteristics of soy globulins as a function of pH and ionic strength. *Colloids Surf A Physicochem Eng Asp* 2007;309:202. <https://doi.org/10.1016/j.colsurfa.2007.01.030>.
- [28] Delahajie RJBM, Gruppen H, Giuseppin MLF, Wierenga PA. Towards predicting the stability of protein-stabilized emulsions. *Adv Colloid Interface Sci* 2015;219:1. <https://doi.org/10.1016/j.cis.2015.01.008>.
- [29] Damodaran S. Protein stabilization of emulsions and foams. *J Food Sci* 2005;70:R54. <https://doi.org/10.1111/j.1365-2621.2005.tb07150.x>.
- [30] Murray BS. Stabilization of bubbles and foams. *Curr Opin Colloid Interface Sci* 2007;12:232. <https://doi.org/10.1016/j.cocis.2007.07.009>.
- [31] Sharma A, Ruckenstein E. Stability, critical thickness, and the time of rupture of thinning foam and emulsion Films. *Langmuir* 1987;3:760. <https://doi.org/10.1021/la00077a033>.
- [32] Mikhailovskaya AA, Noskov BA, Nikitin EA, Lin SY, Loglio G, Miller R. Dilational surface viscoelasticity of protein solutions. Impact of Urea. *Food Hydrocoll* 2014;34:98. <https://doi.org/10.1016/j.foodhyd.2012.12.012>.
- [33] Noskov BA, Grigoriev DO, Latnikova AV, Lin SY, Loglio G, Miller R. Impact of globule unfolding on Dilational viscoelasticity of β -Lactoglobulin adsorption layers. *J Phys Chem B* 2009;113:13398. <https://doi.org/10.1021/jp905413q>.
- [34] Noskov BA, Mikhailovskaya AA, Lin SY, Loglio G, Miller R. Bovine serum albumin unfolding at the air/water Interface as studied by Dilational surface rheology. *Langmuir* 2010;26:17225. <https://doi.org/10.1021/la103360h>.
- [35] Kotsmar C, Pradines V, Alahverdieva VS, Aksenenko EV, Fainerman VB, Kovalchuk VI, et al. Thermodynamics, adsorption kinetics and rheology of mixed protein-surfactant interfacial layers. *Adv Colloid Interface Sci* 2009;150:41. <https://doi.org/10.1016/j.cis.2009.05.002>.
- [36] Mikhailovskaya AA, Noskov BA, Lin SY, Loglio G, Miller R. Formation of protein/surfactant adsorption layer at the air/water Interface as studied by Dilational surface rheology. *J Phys Chem B* 2011;115:9971. <https://doi.org/10.1021/jp204956g>.
- [37] Fruhner H, Wantke KD, Lunkenhheimer K. Relationship between surface Dilational properties and foam stability. *Colloids Surf A Physicochem Eng Asp* 2000;162:193. [https://doi.org/10.1016/S0927-7757\(99\)00202-2](https://doi.org/10.1016/S0927-7757(99)00202-2).
- [38] Coons JE, Halley PJ, McGlashan SA, Tran-Cong T. A review of drainage and spontaneous rupture in free standing Thin Films with tangentially immobile interfaces. *Adv Colloid Interface Sci* 2003;105:3. [https://doi.org/10.1016/S0001-8686\(03\)00003-4](https://doi.org/10.1016/S0001-8686(03)00003-4).
- [39] Ivanov IB, Dimitrov DS. Hydrodynamics of thin liquid Films - effect of surface viscosity on thinning and rupture of foam Films. *Colloid Polym Sci* 1974;252:982. <https://doi.org/10.1007/BF01566619>.
- [40] Manev ED, Sazdanova SV, Wasan DT. Emulsion and foam stability - the effect of film size on film drainage. *J Colloid Interface Sci* 1984;97:591. [https://doi.org/10.1016/0021-9797\(84\)90334-5](https://doi.org/10.1016/0021-9797(84)90334-5).
- [41] Koehler SA, Hilgenfeldt S, Weeks ER, Stone HA. Drainage of single plateau Borders: direct observation of rigid and Mobile interfaces. *Phys Rev E Stat Phys Plasmas Fluids Relat Interdiscip Topics* 2002;66:4. <https://doi.org/10.1103/PhysRevE.66.040601>.
- [42] Stabel A, Heinz R, De Schryver FC, Rabe JP, Ostwald ripening of two-dimensional crystals at the solid-liquid Interface. *J Phys Chem* 1995;99:505. <https://doi.org/10.1021/j100002a009>.
- [43] Hartland S, Bourne JR, Ramaswami S. A study of disproportionation effects in semi-batch foams II. Comparison between experiment and theory. *Chem Eng Sci* 1993;48:1723. [https://doi.org/10.1016/0009-2509\(93\)80131-9](https://doi.org/10.1016/0009-2509(93)80131-9).
- [44] Meinders MBJ, Van Vliet T. The role of interfacial rheological properties on Ostwald ripening in emulsions. *Adv Colloid Interface Sci* 2004;108-109:119. <https://doi.org/10.1016/j.cis.2003.10.005>.

[45] Vrij A. Possible mechanism for the spontaneous rupture of Thin, free liquid films. *Discuss Faraday Soc* 1966;42:23. <https://doi.org/10.1039/DF9664200023>.

[46] Chatzigiannakis E, Jaesson N, Vermant J. Thin liquid Films: where hydrodynamics, capillarity, surface stresses and intermolecular forces meet. *Curr Opin Colloid Interface Sci* 2021;53. <https://doi.org/10.1016/j.cocis.2021.101441>.

[47] Ivanov IB, Radoev B, Manev E, Scheludko A. Theory of the critical thickness of rupture of Thin liquid Films. *Trans Faraday Soc* 1970;66:1262. <https://doi.org/10.1039/TF9706601262>.

[48] Klitzing RV, Müller HJ. Film stability control. *Curr Opin Colloid Interface Sci* 2002;7:42. [https://doi.org/10.1016/S1359-0294\(02\)00005-5](https://doi.org/10.1016/S1359-0294(02)00005-5).

[49] Langevin D. Coalescence in foams and emulsions: similarities and differences. *Curr Opin Colloid Interface Sci* 2019;44:23. <https://doi.org/10.1016/j.cocis.2019.09.001>.

[50] Langevin D, Sonin AA. Thinning of soap Films. *Adv Colloid Interface Sci* 1994;51:1. [https://doi.org/10.1016/0001-8866\(94\)80033-2](https://doi.org/10.1016/0001-8866(94)80033-2).

[51] Manev ED, Angarska JK. Critical thickness of Thin liquid Films: comparison of theory and experiment. *Colloids Surf A Physicochem Eng Asp* 2005;263:250. <https://doi.org/10.1016/j.colsurfa.2004.12.055>.

[52] Qu D, Brotons G, Bosio V, Fery A, Salditt T, Langevin D, et al. Interactions across liquid Thin Films. *Colloids Surf A Physicochem Eng Asp* 2007;303:97. <https://doi.org/10.1016/j.colsurfa.2007.03.055>.

[53] Radoev BP, Scheludko AD, Manev ED. Critical thickness of Thin liquid Films: theory and experiment. *J Colloid Interface Sci* 1983;95:254. [https://doi.org/10.1016/0021-9797\(83\)90094-2](https://doi.org/10.1016/0021-9797(83)90094-2).

[54] Scheludko A. Über das Ausfließen der Lösung aus Schaumfilmen. *Kolloid-Zeitschrift* 1957;155:39. <https://doi.org/10.1007/BF01501293>.

[55] Shelduk A. Thin liquid films. *Adv Colloid Interface Sci* 1967;1:391. [https://doi.org/10.1016/0001-8866\(67\)85001-2](https://doi.org/10.1016/0001-8866(67)85001-2).

[56] Stubenrauch C, Von Klitzing R. Disjoining pressure in Thin liquid foam and emulsion Films - new concepts and perspectives. *J Phys Condens Matter* 2003;15:R1197. <https://doi.org/10.1088/0953-8984/15/27/201>.

[57] Narsimhan G. Characterization of Interfacial Rheology of Protein-Stabilized Air-Liquid Interfaces. *Food Eng Rev* 2016;8:367. <https://doi.org/10.1007/s12393-015-9133-z>.

[58] Dimitrova TD, Leal-Calderon F, Gurkov TD, Campbell B. Disjoining pressure vs thickness isotherms of Thin emulsion Films stabilized by proteins. *Langmuir* 2001;17:8069. <https://doi.org/10.1021/la0111147>.

[59] Charles GE, Mason SG. The coalescence of liquid drops with flat liquid/liquid interfaces. *J Colloid Sci* 1960;15:236. [https://doi.org/10.1016/0095-8522\(60\)90026-X](https://doi.org/10.1016/0095-8522(60)90026-X).

[60] Chatzigiannakis E, Vermant J. Breakup of Thin liquid Films: from stochastic to deterministic. *Phys Rev Lett* 2020;125. <https://doi.org/10.1103/PhysRevLett.125.158001>.

[61] Georgieva D, Cagna A, Langevin D. Link between surface elasticity and foam stability. *Soft Matter* 2009;5:2063. <https://doi.org/10.1039/b822568k>.

[62] Dachmann E, Nobis V, Kulozik U, Dombrowski J. Surface and foaming properties of potato proteins: impact of protein concentration, pH value and ionic strength. *Food Hydrocoll* 2020;107. <https://doi.org/10.1016/j.foodhyd.2020.105981>.

[63] Marinova KG, Stanimirova RD, Georgiev MT, Alexandrov NA, Basheva ES, Krachevsky PA. Co-adsorption of the proteins β -casein and BSA in relation to the stability of Thin liquid films and foams. In: *Colloid and interface chemistry for nanotechnology*; 2016. p. 439–58.

[64] Rouimi S, Schorsch C, Valentini C, Vaslin S. Foam stability and interfacial properties of Milk protein-surfactant systems. *Food Hydrocoll* 2005;19:467. <https://doi.org/10.1016/j.foodhyd.2004.10.032>.

[65] Braunschweig B, Schulze-Zachau F, Nagel E, Engelhardt K, Stoyanov S, Gochev G, et al. Specific effects of Ca^{2+} ions and molecular structure of β -Lactoglobulin interfacial layers that drive macroscopic foam stability. *Soft Matter* 2016;12:5995. <https://doi.org/10.1039/c6sm00636a>.

[66] Delahaye RJBM, Lech FJ, Wierenga PA. Hydrophobicity enhances formation of protein-stabilized foams. *Molecules* 2022;27:2358. <https://doi.org/10.3390/molecules2702358>.

[67] Gochev G, Retzlaff I, Exerowa D, Miller R. Electrostatic stabilization of foam Films from β -Lactoglobulin solutions. *Colloids Surf A Physicochem Eng Asp* 2014;460:272. <https://doi.org/10.1016/j.colsurfa.2013.12.037>.

[68] Schwenzeier A, Lech F, Wierenga PA, Eppink MHM, Gruppen H. Foam properties of algal soluble protein isolate: effect of pH and ionic strength. *Food Hydrocoll* 2013;33:111. <https://doi.org/10.1016/j.foodhyd.2013.03.002>.

[69] Wierenga PA, van Noré L, Basheva ES. Reconsidering the importance of interfacial properties in foam stability. *Colloids Surf A Physicochem Eng Asp* 2009;344:72. <https://doi.org/10.1016/j.colsurfa.2009.02.012>.

[70] Wilde PJ. Interfaces: their role in foam and emulsion behaviour. *Curr Opin Colloid Interface Sci* 2000;5:176. [https://doi.org/10.1016/S1359-0294\(00\)00056-X](https://doi.org/10.1016/S1359-0294(00)00056-X).

[71] Ulaganathan V, Retzlaff I, Won JY, Gochev G, Gunes DZ, Gehin-Delval C, et al. β -lactoglobulin adsorption layers at the water/air surface 2. Dilatational rheology effect of pH and ionic strength. *Colloids Surf A Physicochem Eng Asp* 2017;521:167. <https://doi.org/10.1016/j.colsurfa.2016.08.064>.

[72] Noskov BA, Akentiev AV, Bilibin AY, Zorin IM, Miller R. Dilatational surface viscoelasticity of polymer solutions. *Adv Colloid Interface Sci* 2003;104:245. [https://doi.org/10.1016/S0001-8686\(03\)00045-9](https://doi.org/10.1016/S0001-8686(03)00045-9).

[73] Samanta S, Ghosh P. Coalescence of bubbles and stability of foams in aqueous solutions of tween surfactants. *Chem Eng Res Des* 2011;89:2344. <https://doi.org/10.1016/j.cherd.2011.04.006>.

[74] Samanta S, Ghosh P. Coalescence of air bubbles in aqueous solutions of alcohols and nonionic surfactants. *Chem Eng Sci* 2011;66:4824. <https://doi.org/10.1016/j.ces.2011.06.046>.

[75] Szekrényesy T, Liktor K, Sándor N. Characterization of foam stability by the use of foam models 1. Models and derived lifetimes. *Colloids Surf* 1992;68:267. [https://doi.org/10.1016/0166-6622\(92\)80212-K](https://doi.org/10.1016/0166-6622(92)80212-K).

[76] Basheva ES, Gurkov TD, Ivanov IB, Bantchev GB, Campbell B, Borwankar RP. Size dependence of the stability of emulsion drops pressed against a large Interface. *Langmuir* 1999;15:6764. <https://doi.org/10.1021/la990186j>.

[77] Rullier B, Axelos MAV, Langevin D, Novales B. β -Lactoglobulin aggregates in foam Films: correlation between foam Films and foaming properties. *J Colloid Interface Sci* 2009;336:750. <https://doi.org/10.1016/j.jcis.2009.04.034>.

[78] Rullier B, Axelos MAV, Langevin D, Novales B. β -Lactoglobulin aggregates in foam Films: effect of the concentration and size of the protein aggregates. *J Colloid Interface Sci* 2010;343:330. <https://doi.org/10.1016/j.jcis.2009.11.015>.

[79] Stubenrauch C, Miller R. Stability of foam Films and surface rheology: an oscillating bubble study at low frequencies. *J Phys Chem B* 2004;108:6412. <https://doi.org/10.1021/jp049694e>.

[80] Langevin D. On the rupture of Thin Films made from aqueous surfactant solutions. *Adv Colloid Interface Sci* 2020;275. <https://doi.org/10.1016/j.cis.2019.102075>.

[81] Politova N, Tcholakova S, Denkov ND. Factors affecting the stability of water-oil-water emulsion Films. *Colloids Surf A Physicochem Eng Asp* 2017;522:608. <https://doi.org/10.1016/j.colsurfa.2017.03.055>.

[82] Gurkov TD, Angarska JK, Tachev KD, Gaschler W. Statistics of rupture in relation to the stability of Thin liquid Films with different size. *Colloids Surf A Physicochem Eng Asp* 2011;382:174. <https://doi.org/10.1016/j.colsurfa.2010.12.010>.

[83] Manev E, Scheludko A, Exerowa D. Effect of surfactant concentration on the critical thicknesses of liquid Films. *Colloid Polym Sci* 1974;252:586. <https://doi.org/10.1007/BF01558157>.

[84] Vakarelski IU, Manica R, Li EQ, Basheva ES, Chan DYC, Thoroddsen ST. Coalescence dynamics of Mobile and immobile fluid interfaces. *Langmuir* 2018;34:2096. <https://doi.org/10.1021/acs.langmuir.7b04106>.

[85] Anachkov SE, Danov KD, Basheva ES, Kralchevsky PA, Ananthapadmanabhan KP. Determination of the aggregation number and charge of ionic surfactant micelles from the stepwise thinning of foam Films. *Adv Colloid Interface Sci* 2012;183:184:55. <https://doi.org/10.1016/j.cis.2012.08.003>.

[86] Nikolov AD, Wasan DT. Ordered micelle structuring in Thin Films formed from anionic surfactant solutions. I experimental. *J Colloid Interface Sci* 1989;133:1. [https://doi.org/10.1016/0021-9797\(89\)90278-6](https://doi.org/10.1016/0021-9797(89)90278-6).

[87] von Klitzing R, Thormann E, Nylander T, Langevin D, Stubenrauch C. Confinement of linear polymers, surfactants, and particles between interfaces. *Adv Colloid Interface Sci* 2010;155:19. <https://doi.org/10.1016/j.cis.2010.02.003>.

[88] Evans DE, Oberdieck M, Redd KS, Newman R. Comparison of the Rudin and NIBEM methods for measuring foam stability with a manual pour method to identify beer characteristics that deliver consumers stable beer foam. *J Am Soc Brew Chem* 2012;70:70. <https://doi.org/10.1094/ASBCJ-2012-1205-01>.

[89] Wallin CE, DiPietro MB, Schwarz RW, Bamforth CW. A comparison of three methods for the assessment of foam stability of beer. *J Inst Brewing* 2010;116:78. <https://doi.org/10.1002/j.2050-0416.2010.tb00401.x>.

[90] Evans DE, Bamforth CW. Beer foam: achieving a suitable head. *Beer* 2009;1–60.

[91] Evans DE, Surrel A, Sheehy M, Stewart DC, Robinson LH. Comparison of foam quality and the influence of hop α -acids and proteins using five foam analysis methods. *J Am Soc Brew Chem* 2008;66:1. <https://doi.org/10.1094/ASBCJ-2007-1129-01>.

[92] Kosin P, Savel J, Evans DE, Broz A. Relationship between matrix foaming potential, beer composition, and foam stability. *J Am Soc Brew Chem* 2010;68:63. <https://doi.org/10.1094/ASBCJ-2010-0114-01>.

[93] Iimure T, Takoi K, Kaneko T, Kihara M, Hayashi K, Ito K, et al. Novel prediction method of beer foam stability using protein Z, barley dimeric α -amylase Inhibitor-1 (BDAI-1) and yeast Thiorodoxin. *J Agric Food Chem* 2008;56:8664. <https://doi.org/10.1021/jf801184k>.

[94] Lu Y, Bergenstahl B, Nilsson L. Interfacial properties and interaction between beer wort protein fractions and Iso-Humulone. *Food Hydrocoll* 2020;103. <https://doi.org/10.1016/j.foodhyd.2020.105648>.

[95] Van Nierop SNE, Evans DE, Axcell BC, Cantrell IC, Rautenbach M. Impact of different wort boiling temperatures on the beer foam stabilizing properties of lipid transfer protein 1. *J Agric Food Chem* 2004;52:3120. <https://doi.org/10.1021/f035125c>.

[96] Krycki MM, Lin SY, Loglio G, Michailov AV, Miller R, Noskov BA. Impact of denaturing agents on surface properties of myoglobin solutions. *Colloids Surf B Biointerfaces* 2021;202. <https://doi.org/10.1016/j.colsurfb.2021.111657>.

[97] Hawks SE, Phillips LG, Rasmussen RR, Barbano DM, Kinsella JE. Effects of processing treatment and cheese-making parameters on foaming properties of whey protein isolates. *J Dairy Sci* 1993;76:2468. [https://doi.org/10.3168/jds.S0022-0302\(93\)77581-5](https://doi.org/10.3168/jds.S0022-0302(93)77581-5).

[98] Coons JE, Halley PJ, McGlashan SA, Tran-Cong T. Scaling Laws for the critical rupture thickness of common Thin Films. *Colloids Surf A Physicochem Eng Asp* 2005;263:258. <https://doi.org/10.1016/j.colsurfa.2005.01.008>.

[99] Wierenga PA, Basheva ES, Denkov ND. Modified capillary cell for foam film studies allowing exchange of the film-forming liquid. *Langmuir* 2009;25:6035. <https://doi.org/10.1021/la901068w>.

[100] Fainerman VB, Miller R, Ferri JK, Watzke H, Leser ME, Michel M. Reversibility and irreversibility of adsorption of surfactants and proteins at liquid interfaces. *Adv Colloid Interface Sci* 2006;123-126:163. <https://doi.org/10.1016/j.cis.2006.05.023>.

[101] Ferri JK, Gorevski N, Kotsmar C, Leser ME, Miller R. Desorption kinetics of surfactants at fluid interfaces by novel coaxial capillary pendant drop experiments. *Colloids Surf A Physicochem Eng Asp* 2008;319:13. <https://doi.org/10.1016/j.colsurfa.2007.07.037>.

[102] Svitova TF, Radke CJ. AOT and Pluronic F68 Coadsorption at fluid/fluid interfaces: a continuous-flow Tensiometry study. *Ind Eng Chem Res* 2005;44: 1129. <https://doi.org/10.1021/ie049676j>.

[103] Engelhardt K, Rumpel A, Walter J, Dombrowski J, Kulozik U, Braunschweig B, et al. Protein adsorption at the electrified air-water Interface: implications on foam stability. *Langmuir* 2012;28:7780. <https://doi.org/10.1021/la301368v>.

[104] Engelhardt K, Lexis M, Gochev G, Konnerth C, Miller R, Willenbacher N, et al. pH effects on the molecular structure of β -Lactoglobulin modified air-water interfaces and its impact on foam rheology. *Langmuir* 2013;29:11646. <https://doi.org/10.1021/la402729g>.

[105] Qiao X, Miller R, Schneck E, Sun K. Foaming properties and the dynamics of adsorption and surface rheology of silk fibroin at the air/water Interface. *Colloids Surf A Physicochem Eng Asp* 2020;591:124553. <https://doi.org/10.1016/j.colsurfa.2020.124553>.

[106] Gochev GG, Scoppola E, Campbell RA, Noskov BA, Miller R, Schneck E. β -Lactoglobulin adsorption layers at the air/water surface: 3. Neutron reflectometry study on the effect of pH. *J Phys Chem B* 2019;123:10877. <https://doi.org/10.1021/acs.jpcb.9b07733>.

[107] Pasquier C, Pezennec S, Bouchoux A, Cabane B, Lechevalier-Datin V, Le Floch-Fouéré C, et al. Protein transport upon advection at the air/water Interface: when charge matters. *Langmuir* 2021;37:12278. <https://doi.org/10.1021/acs.langmuir.1c01591>.

[108] Pahl R, Meyer B, Biurrun R. Wort and wort quality parameters. In: *Brewing materials and processes: a practical approach to beer excellence*; 2016. p. 113–21.

[109] Gawel D, Zawala J. Stability of liquid Films formed by a single bubble and droplet at liquid/gas and liquid/liquid interfaces in bovine serum albumin solutions. *ACS Omega* 2021;6:18289. <https://doi.org/10.1021/acsomega.1c02188>.

[110] Ghosh P. A comparative study of the film-drainage models for coalescence of drops and bubbles at flat Interface. *Chem Eng Technol* 2004;27:1200. <https://doi.org/10.1002/ceat.200402143>.

[111] Ghosh P. Coalescence of air bubbles at air-water Interface. *Chem Eng Res Des* 2004;82:849. <https://doi.org/10.1205/0263876041596715>.

[112] Wierenga PA, Meinders MBJ, Egmond MR, Voragen AGJ, De Jongh HHJ. Quantitative description of the relation between protein net charge and protein adsorption to air-water interfaces. *J Phys Chem B* 2005;109:16946. <https://doi.org/10.1021/jp050990g>.

[113] Kotsmár C, Grigoriev DO, Makievski AV, Ferri JK, Krägel J, Miller R, et al. Drop profile analysis Tensiometry with drop bulk exchange to study the sequential and simultaneous adsorption of a mixed β -casein/ C12DMPO system. *Colloid Polym Sci* 2008;286:1071. <https://doi.org/10.1007/s00396-008-1872-4>.

[114] Ball V, Ramsden JJ. Buffer dependence of refractive index increments of protein solutions. *Biopolymers* 1998;46:489. [https://doi.org/10.1002/\(SICI\)1097-0282\(199812\)46:7<489::AID-BIP6>3.0.CO;2-E](https://doi.org/10.1002/(SICI)1097-0282(199812)46:7<489::AID-BIP6>3.0.CO;2-E).

[115] De Feijter JA, Benjamins J, Veer FA. Ellipsometry as a tool to study the adsorption behavior of synthetic and biopolymers at the air–water interface. *Biopolymers* 1978;17:1759. <https://doi.org/10.1002/bip.1978.360170711>.

[116] Erni P, Fischer P, Windhab EJ, Kusnezov V, Stettini H, Läuger J. Stress- and strain-controlled measurements of interfacial shear viscosity and viscoelasticity at liquid/liquid and gas/liquid interfaces. *Rev Sci Instrum* 2003;74:4916. <https://doi.org/10.1063/1.1614433>.

[117] Scheludko A, Exerowa D. Über den elektrostatischen Druck in Schaumfilmen aus wässrigeren Elektrolytlösungen. *Kolloid-Zeitschrift* 1959;165:148. <https://doi.org/10.1007/BF01809974>.

[118] Velev OD, Constantinides GN, Avraam DG, Payatakes AC, Borwankar RP. Investigation of Thin liquid Films of small diameters and high capillary pressures by a miniaturized cell. *J Colloid Interface Sci* 1995;175:68. <https://doi.org/10.1006/jcis.1995.1430>.

[119] Lech FJ, Wierenga PA, Gruppen H, Meinders MBJ. Stability properties of surfactant-free Thin Films at different ionic strengths: measurements and modeling. *Langmuir* 2015;31:2777. <https://doi.org/10.1021/la504933e>.

[120] Joye JL, Miller CA, Hirasaki GJ. Dimple formation and behavior during Axisymmetrical foam film drainage. *Langmuir* 1992;8:3083. <https://doi.org/10.1021/la00048a038>.

[121] Mysels KJ. Soap Films and some problems in surface and colloid chemistry. *J Phys Chem* 1964;68:3441. <https://doi.org/10.1021/j100794a001>.

[122] Danov KD, Basheva ES, Kralchevsky PA. Effect of ionic correlations on the surface forces in Thin liquid Films: influence of multivalent Coions and extended theory. *Materials* 2016;9. <https://doi.org/10.3390/ma9030145>.

[123] Mysels KJ, Jones MN. Direct measurement of the variation of double-layer repulsion with distance. *Discuss Faraday Soc* 1966;42:42. <https://doi.org/10.1039/DF9664200042>.